Sol−Gel Processed Phosphine Ligands with Two T- or D-Silyl Functionalities and Their (η^5-C_5Me_5)Ru(II) Complexes[1]

Ekkehard Lindner,*,† Wolfram Wielandt,† Andreas Baumann,† Hermann A. Mayer,† Ulrich Reinöhl,‡ Achim Weber,‡ Teja S. Ertel,‡ and Helmut Bertagnolli‡

Institut für Anorganische Chemie der Universität, Auf der Morgenstelle 18, D-72076 Tübingen, and Institut für Physikalische Chemie der Universität Stuttgart, Pfaffenwaldring 55, D-70569 Stuttgart, Germany

Received January 26, 1999. Revised Manuscript Received April 15, 1999

A new class of hemilabile D- and T-functionalized ether phosphine ligands of the type $MeOCH_2CH_2P[(CH_2)_zSiMe_m(OMe)_{3-m}]_2$ [**3a,b,d,e(T^0)** (m = 0: z = 3 (**a**), 6 (**b**), 8 (**d**), 14 (**e**)), and **3c(D^0)** (m = 1; z = 6 (**c**))] was obtained by treatment of 2-methoxyethylphosphine (**1**) with the ω-alkenylsilanes $H_2C{=}CH(CH_2)_zSiMe_m(OMe)_{3-m}$ (**2a**−**e**). Treatment of [(η^5-C_5Me_5)-$RuCl]_4$ with the T-silyl phosphines **3a,b,d,e(T^0)** results in the formation of the corresponding complexes (η^5-C_5Me_5)$RuCl\{MeOCH_2CH_2P[(CH_2)_zSiMe_m(OMe)_{3-m}]_2\}_2$ [**4a,b,d,e(T^0)**]. In the presence of CH_3CN and $AgSbF_6$ **4b(T^0)** affords the cationic T-silyl complex [(η^5-C_5Me_5)$Ru(NCCH_3)\{MeOCH_2CH_2P[(CH_2)_6SiMe_m(OMe)_{3-m}]_2\}_2]^+SbF_6^-$ [**5b(T^0)**]. **3a,b,d,e(T^0)**, **3c(D^0)**, **4a,b,d,e(T^0)**, and **5b(T^0)** were sol−gel processed with variable amounts of the co-condensation agent $(MeO)_2MeSi(CH_2)_6SiMe(OMe)_2$ (**D^0**−**C$_6$**−**D^0**) to give the stationary phases (Fn = functionality → ligands or complexes) $\{Fn[SiO_{n/2}(OX)_{3-n}]_2\}\{MeSiO_{i/2}(OX)_{2-i}(CH_2)_6(XO)_{2-i}$-$O_{i/2}SiMe\}_y$, Fn = $P(CH_2CH_2OMe)[(CH_2)_z-]_2$ [**3a,b,d,e(T^n)$_2$(D^i**−**C$_6$**−**D^i)$_y$** ≙ **I$_1$**, **II$_0$**−**II$_4$**, **IV$_1$**, **V$_1$**], $\{Fn[SiO_{i/2}(OX)_{2-i}Me]_2\}\{MeSiO_{i/2}(OX)_{2-i}(CH_2)_6(XO)_{2-i}O_{i/2}SiMe\}_4$ [**3c(D^i)$_2$(D^i**−**C$_6$**−**D^i)$_4$** ≙ **III$_4$**], Fn = $[Cp^*RuCl]_{1/2}P(CH_2CH_2OMe)[(CH_2)_z-]_2$ [**4a,b,d,e(T^n)$_4$(D^i**−**C$_6$**−**D^i)$_y$** ≙ **VI$_1$**, **VII$_0$**, **VII$_1$**, **VIII$_1$**, **IX$_1$**], and Fn = $\{[Cp^*Ru(NCCH_3)]^+SbF_6^-\}_{1/2}P(CH_2CH_2OMe)[(CH_2)_6-]_2$ [**5b(T^n)$_4$-(D^i**−**C$_6$**−**D^i)$_4$** ≙ **X$_4$**] (see Table 1) [T = T-type silicon atom (three oxygen neighbors); D = D-type silicon atom (two oxygen neighbors); n, i = number of Si−O−Si bonds; n = 0−3, i = 0−2; y = number of co-condensed **D^0**−**C$_6$**−**D^0** molecules]. Realistic amounts of T and D species and the degree of condensation were determined ^{29}Si CP/MAS NMR spectroscopically. The polymeric phosphines **I$_1$**, **II$_0$**−**II$_4$**, **IV$_1$**, and **V$_1$** show higher degrees of condensation than the corresponding ruthenium(II) complexes **VI$_1$**, **VII$_0$**, **VII$_1$**, **VIII$_1$**, and **IX$_1$**. Bond lengths of the ruthenium(II) complex in the stationary phase **VII$_0$** were elucidated by an EXAFS analysis. From relaxation time studies (T_{1P}, $T_{1\rho H}$) and cross-polarization experiments (T_{PH}), it is concluded that the polymeric phosphines **I$_1$**, **II$_0$**−**II$_4$**, **IV$_1$**, and **V$_1$** reveal an increasing mobility with longer alkyl spacers between the polymer and the P-functionality and an increasing amount of the co-condensation agent **D^0**−**C$_6$**−**D^0**. Owing to the multiple fixation of the ruthenium centers to the polymeric matrixes in the stationary phases **VI$_1$**, **VII$_0$**, **VII$_1$**, **VIII$_1$**, **IX$_1$**, and **X$_4$**, the mobility in these materials is reduced. ^{1}H,^{13}C-2D-WISE NMR investigations on the interphase set up by **X$_4$** and EtOH point to a remarkable decrease of the rigid character compared to the stationary phase **X$_4$** without EtOH.

Introduction

In catalytic processes, the separation of products from the catalyst represents a crucial step for the recycling of the catalyst containing precious metals.[2] To overcome this problem, several concepts have been developed in the past or are still under investigation.[3] A typical example is biphasic catalysis which attained application in the so-called Ruhrchemie/Rhône-Poulenc oxo process.[4] However, this technique cannot be transferred to higher olefins due to their complete insolubility in water. Another approach considers the immobilization of homogeneous catalysts.[5,6] The anchoring of reactive centers at inorganic or organic polymers entails several momentous disadvantages such as high metal loss

* Corresponding author. E-mail: ekkehard lindner@uni-tuebingen.de.
† Institut für Anorganische Chemie der Universität Tübingen.
‡ Institut für Physikalische Chemie der Universität Stuttgart.

(1) Supported Organometallic Complexes. Part 18. Part 17: Lindner, E.; Jäger, A.; Wegner, P.; Mayer, H. A.; Benez, A.; Adam, D.; Plies, E. *J. Non-Cryst. Solids*, in press.
(2) Hagen, J. *Technical Catalysis*; VCH: Weinheim, Germany, 1996.
(3) Lindner, E.; Schneller, T.; Auer, F.; Mayer, H. A. *Angew. Chem., Int. Ed. Engl.*, in press.
(4) (a) Wiebus, E.; Cornils, B. *Chem. Ing. Technol.* **1994**, *66*, 916. (b) Cornils, B.; Wiebus, E. *CHEMTECH* **1995**, 33.
(5) Hartley, F. R. *Supported Metal Complexes*; D. Reidel Publishing Company: Dordrecht, The Netherlands, 1985.
(6) Schubert, U. *New J. Chem.* **1994**, *18*, 1049.

10.1021/cm9900498 CCC: $18.00
Published on Web 06/17/1999

("leaching") or inhomogeneity of the reactive centers.[7] As an efficient alternative for the reduction or even elimination of these handicaps, *chemistry in interphases* was recently introduced.[8] An interphase is established if a stationary phase (polymer + spacer + reactive center) and a mobile component (solvent, gaseous, liquid, or dissolved reactant) penetrate each other on a molecular scale without forming a homogeneous phase. By employing well-designed, sol−gel processed hybrid polymers such as polysiloxanes,[9−12] leaching is reduced to a markable extent. As an unrenounceable precondition, the polymeric matrix has to reveal high swelling abilities in the presence of a mobile phase. This is realized by introduction of suitable co-condensation agents and an adequate spacer length.[13,14] In such a case, a high mobility is achieved which is necessary for the accessibility of the reactive centers by substrates.[15]

To avoid leaching for reactions in interphases, the reactive centers have to be effectively embedded into the polysiloxane backbone. Functionalized phosphines with appropriately designed substituents at the phosphorus atoms have proved to meet this requirement.[16−18] This is verified on one hand by a strong metal−phosphorus bond, which is attained if the phosphorus atoms are provided with three alkyl groups, and on the other hand by fixation of the P-ligand to the polymer via two spacer units.[19] However, such a "double fixation" of the reactive centers to the polymer matrix leads to a reduced flexibility and hence to a less active catalyst. To compensate this drawback, different spacer lengths of up to 14 methylene groups with modified silyl functions have been introduced into the ligand system[20] and specific amounts of co-condensation agents were applied.

For several years, hemilabile ether phosphines have been extensively investigated in organometallic chemistry[21] as a tool to stabilize empty coordination sites at reactive centers. In this way, weak metal−oxygen bonds are formed which are cleaved reversibly. Herein the ether moiety functions as an intramolecular solvent. In the presence of reactants, weakly protected coordination sites are made available for the activation of catalytically relevant small molecules.[22]

Herein we wish to report on a facile synthetic approach to novel achiral, sol−gel applicable phosphine ligands with two spacer units and one ether function. To ensure the utility of these ligands in metal complexes with potentially catalytic activity, (η^5-C_5Me_5)Ru(II) complexes were generated and subjected to a sol−gel process. A detailed and comparative characterization of the resulting polymeric ligands and complexes as stationary phases by solid-state NMR spectroscopy illustrates the mobility of these polymers in dependence on the spacer length, silyl species, and employed co-condensation agent. Some of the new materials were also investigated exemplarily by EXAFS and SEM measurements.

Results and Discussion

Monomeric Phosphine Ligands 3a,b,d,e(T^0) and 3c(D^0). A less toxic and more straightforward method than that described in the literature[23] for the access of the primary phosphine $H_2P(CH_2)_2OMe$ (**1**) is the reduction of the phosphonate $(EtO)_2P(O)(CH_2)_2OMe$ with $LiAlH_4$ in di-*n*-butyl ether (Scheme 1).[24−26] Compound **1** represents a colorless, bad-smelling liquid revealing a singlet in the $^{31}P\{^1H\}$ NMR spectrum. The occurrence of two doublets and one singlet in the $^{13}C\{^1H\}$ NMR spectrum is ascribed to the methylene and methoxy carbon atoms. The trialkylphosphines $[Me_m(MeO)_{3-m}Si(CH_2)_z]_2P(CH_2)_2OMe$ [**3a,b,d,e(T^0)** ($m = 0$; $z = 3$, 6, 8, 14) and **3c(D^0)** ($m = 1$; $z = 6$)] fail to form upon treatment of the lithiated or chlorinated phosphine **1** with ω-bromoalkylalkoxysilanes or their Grignard derivatives, respectively, because the corresponding silane is sensitive to basic reagents. A different route to generate P−C bonds is the photochemically or radically induced hydrophosphination of unsaturated hydrocarbons with P−H functions.[27,28] This procedure operates well to afford the phosphine ligands **3a,b,d,e(T^0)** and **3c(D^0)** as colorless oily products which are rather sensitive to oxygen and moisture (Scheme 1). Their composition was established by mass spectra displaying the expected molecular peak in each case. From the $^{13}C\{^1H\}$ NMR spectra it is concluded that both silylalkyl functions are equivalent since only one resonance is observed for each methylene carbon atom. Up to the third methylene group following the phosphorus atom, the ^{13}C signals are split into doublets. The ^{13}C signals observed at higher field (<11 ppm) are attributed to the CH_2 units adjacent to silicon. Resonances at δ 68 (doublet) and 56 (singlet) corroborate that the 2-methoxyethyl ether substituents are still intact.

Monomeric (η^5-C_5Me_5)Ru(II) Complexes 4a,b,d,e(T^0) and 5b(T^0). Treatment of the starting complex $[(\eta^5\text{-}C_5Me_5)Ru(\mu_3\text{-}Cl)]_4$[29] with the phosphine ligands **3a,b,d,e-**

(7) Khatib, I. S.; Parish, R. V. *J. Organomet. Chem.* **1989**, *369*, 9.
(8) Lindner, E.; Schreiber, R.; Kemmler, M.; Schneller, T.; Mayer, H. A. *Chem. Mater.* **1995**, *7*, 951.
(9) Brinker, C. J.; Scherer, G. W. *Sol-Gel Science*; Academic Press: London, 1990.
(10) Sanchez, C.; Ribot, F. *New J. Chem.* **1994**, *18*, 1007.
(11) Corriu, R.; Leclercq, D. *Angew. Chem., Int. Ed. Engl.* **1996**, *35*, 1420.
(12) Hench, L. L.; West, J. K. *Chem. Rev.* **1990**, *90*, 33.
(13) Shea, K. J.; Loy, D. A.; Webster, O. *J. Am. Chem. Soc.* **1992**, *114*, 6700.
(14) Lindner, E.; Schneller, T.; Mayer, H. A.; Bertagnolli, H.; Ertel, T. S.; Hörner, W. *Chem. Mater.* **1997**, *9*, 1524.
(15) Lindner, E.; Schneller, T.; Auer, F.; Wegner, P.; Mayer, H. A. *Chem. Eur. J.* **1997**, *3*, 1833.
(16) Parish, R. V.; Habibi, D.; Mohammadi, V. *J. Organomet. Chem.* **1989**, *369*, 17.
(17) Deschler, U.; Kleinschmit, P.; Panster, P. *Angew. Chem., Int. Ed. Engl.* **1986**, *25*, 236.
(18) Lindner, E.; Enderle, A.; Baumann, A. *J. Organomet. Chem.* **1998**, *558*, 235.
(19) Panster, P. *Chem. Lab. Biotech.* **1992**, *43*, 16.
(20) Lindner, E.; Jäger, A.; Schneller, T.; Mayer, H. A. *Chem. Mater.* **1997**, *9*, 81.
(21) Bader, A.; Lindner, E. *Coord. Chem. Rev.* **1991**, *108*, 27.
(22) Lindner, E.; Pautz, S.; Haustein, M. *Coord. Chem. Rev.* **1996**, *155*, 145.
(23) N. V. de Bataafsche Petroleum Maatschappij. Br. Patent 673, 451, 1952; *Chem. Abstr.* **1953**, *47*, 5426b.
(24) Horner, L.; Hoffmann, H.; Beck, P. *Chem. Ber.* **1958**, *91*, 1583.
(25) Pass, F.; Schindlbauer, H. *Monatsh. Chem.* **1959**, *90*, 148.
(26) Maier, L. *Helv. Chim. Acta* **1965**, *48*, 1190.
(27) Chadwell, S. J.; Coles, S. J.; Edwards, P. G.; Hursthouse, M. B.; Imran, A. *Polyhedron* **1995**, *14*, 1057.
(28) Wolfberger, W.; Bank, J.; Werner, H. *Z. Naturforsch. B* **1995**, *50*, 1319.
(29) Fagan, P. J.; Ward, M. D.; Calabrese, J. C. *J. Am. Chem. Soc.* **1989**, *111*, 1698.

Scheme 1

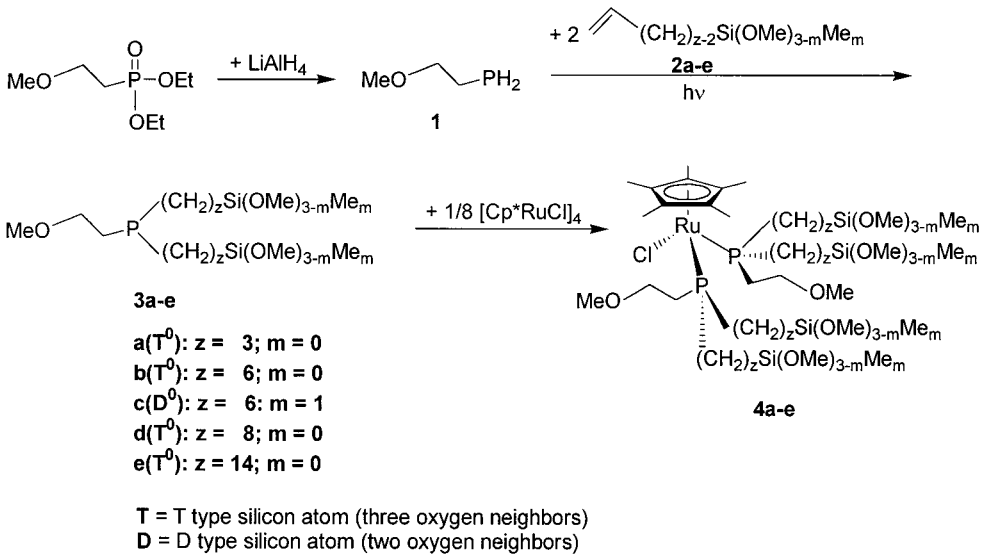

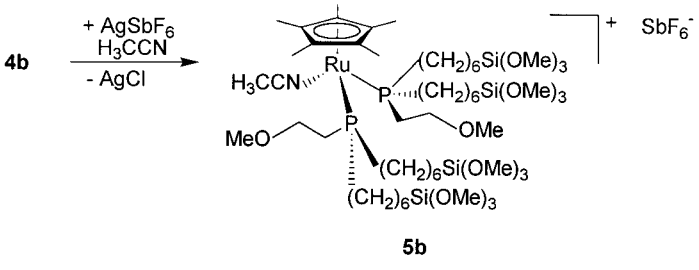

(T⁰) in CH_2Cl_2 results in the formation[30−32] of the highly viscous, brown oils of the monomeric ruthenium(II) complexes (η^5-C_5Me_5)RuCl{$MeOCH_2CH_2P[(CH_2)_zSiMe_m(OMe)_{3-m}]_2$}$_2$ [**4a,b,d,e(T⁰)**] (Scheme 1), which decompose within a week even under an atmosphere of argon. Their composition was verified by the occurrence of the respective molecular peaks in the FD mass spectra. Singlets in the $^{31}P\{^1H\}$ NMR spectra indicate the chemical equivalence of the phosphines. The $^{13}C\{^1H\}$ NMR spectra of the complexes **4a,b,d,e(T⁰)** show three A parts of *AXX′* spin patterns[33] for the phosphorus adjacent methylene groups, which are reduced to three singlets by ^{31}P decoupling. Two additional ^{13}C singlets at δ 87 and 11 are characteristic for the (η^5-C_5Me_5) fragment of the complexes.[34]

The replacement of a chloro ligand by acetonitrile[35] in the presence of $AgSbF_6$ was demonstrated in the case of **4b(T⁰),** resulting in the cationic complex [(η^5-C_5Me_5)-Ru($NCCH_3$){$MeOCH_2CH_2P[(CH_2)_6Si(OMe)_3]_2$}$_2$$^+SbF_6^-$ [**5b(T⁰)**]. The ruthenium complex was characterized by FD-MS, IR, $^{31}P\{^1H\}$, and $^{13}C\{^1H\}$ NMR spectroscopy (see Experimental Section).

Sol−Gel Processing of the Phosphines 3a,b,d,e-(T⁰) and 3c(D⁰) and Complexes 4a,b,d,e(T⁰) and 5b-(T⁰). The properties of sol−gel processed materials strongly depend on the reaction conditions such as concentration of the starting monomers, type and amount of solvent, temperature, reaction time, drying conditions of the wet gel, and type of catalyst.[9] To ensure comparable results, the adherence to uniform reaction conditions has to be maintained during hydrolysis and polycondensation. The employment of (n-Bu)$_2$Sn(OAc)$_2$ as a catalyst offers the advantage of avoiding decomposition of the phosphines **3a,b,d,e(T⁰)** and **3c(D⁰)**. Methanol is necessary to homogenize the reaction mixture. In the case of **3e(T⁰)**, no homogeneity was achieved since the solubility of this T^0 silyl monomer is reduced due to the long alkyl spacers. Upon polycondensation of **3a,b,d,e(T⁰)** and **3c(D⁰)** with different amounts of the co-condensation agent **D−C₆−D**[14] (Scheme 2), white powders are isolated with high swelling abilities in organic solvents. In CH_2Cl_2, the powders form a milky suspension which cannot be separated into two different phases even after several hours. This property is independent of the spacer length, the type of the silyl function of the monomeric ligand, and the amount of the co-condensation agent **D−C₆−D**. The basicity of the monomeric trialkylphosphines accounts for a remarkable sensitivity of the polymers toward oxygen, even in the dry state.

According to these boundary conditions, two types of polysiloxanes with and without co-condensation agents were prepared (Scheme 3). To be sure that the integrity

(30) Campion, C. K.; Heyn, R. H.; Don Tilley, T. *J. Chem. Soc., Chem. Commun.* **1988**, 278.
(31) Jia, G. Lough, A. J.; Morris, R. H. *Organometallics* **1992**, *11*, 161.
(32) Braun, T.; Steinert, P.; Werner, H. *J. Organomet. Chem.* **1995**, *488*, 169.
(33) Harris, R. K. *Can. J. Chem.* **1964**, *42*, 2275.
(34) Lindner, E.; Haustein, M.; Mayer, H. A.; Kühbauch, H.; Vrieze, K.; de Klerk-Engels, B. *Inorg. Chim. Acta* **1994**, *215*, 165.
(35) Lindner, E.; Pautz, S.; Fawzi, R.; Steimann, M. *J. Organomet. Chem.* **1998**, *555*, 247.

Scheme 2

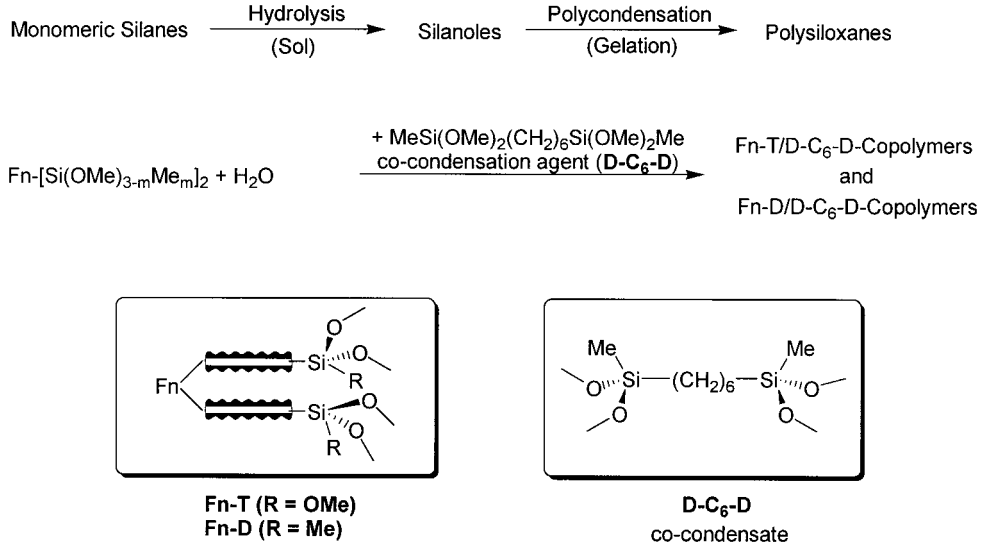

Fn (functionality) = $P(CH_2CH_2OMe)[(CH_2)_z\text{-}]_2$ [**3a,b,d,e(T^0)**; **3c(D^0)**]
Fn (functionality) = $[Cp^*RuCl]_{1/2}P(CH_2CH_2OMe)[(CH_2)_z\text{-}]_2$ [**4a,b,d,e(T^0)**]
Fn (functionality) = $\{[Cp^*Ru(NCCH_3)]^+SbF_6^-\}_{1/2}P(CH_2CH_2OMe)[(CH_2)_z\text{-}]_2$ [**5b(T^0)**]
T = T type silicon atom (three oxygen neighbors)
D = D type silicon atom (two oxygen neighbors)
z = length of the $-CH_2-$ chain [z = 3, 6, 8, 14]

of the phosphine ligands is maintained during the sol−gel process, the T-functionalized phosphine **3b(T^0)** was sol−gel processed without any co-condensation agent leading to **3b(T^n)$_2$** (≙**II$_0$**, Table 1). The Fn−T/D−C_6−D (Fn = functionality → ligands or complexes) copolymers were obtained by co-condensation of the monomers **3a,b,d,e(T^0)** with variable amounts of **D−C$_6$−D**, selecting the T/D stoichiometry of 1:1.

The resulting polymers **3a(T^n)$_2$(D^i−C$_6$−D^i)** (≙**I$_1$**), **3b(T^n)$_2$(D^i−C$_6$−D^i)** (≙**II$_1$**), **3d(T^n)$_2$(D^i−C$_6$−D^i)** (≙**IV$_1$**), and **3e(T^n)$_2$(D^i−C$_6$−D^i)** (≙**V$_1$**, Table 1) were investigated to obtain information about the influence of the different spacer units on the mobility of the phosphorus atoms in the polymeric system.[20] Furthermore, the contribution of higher stoichiometric amounts of **D−C$_6$−D** to the flexibility of the polymer was studied by the preparation of the polysiloxanes **3b(T^n)$_2$(D^i−C$_6$−D^i)$_2$** (≙**II$_2$**), **3b(T^n)$_2$(D^i−C$_6$−D^i)$_4$** (≙**II$_4$**), and **3c(D^i)$_2$(D^i−C$_6$−D^i)$_4$** (≙**III$_4$**) with T/D and D/D ratios of 1:2 and 1:4, respectively. Comparisons between the polymers **II$_4$** and **III$_4$** (Table 1) render possible information about whether different silyl functions at the ends of a spacer modify the properties of the polysiloxanes. Since in sol−gel processes normally the Si−OH groups are condensed incompletely, excess water has to be employed to achieve a high degree of hydrolysis. All prepared polysiloxanes are summarized in Table 1; idealized and realistic compositions of the polycondensation products are depicted in Scheme 4.

The instability of the monomeric precursors **4a,b,d,e(T^0)** requires a sol−gel polycondensation temperature of −20 °C. In this way, the yellow-brown polymers **4a(T^n)$_4$(D^i−C$_6$−D^i)** (≙**VI$_1$**), **4b(T^n)$_4$(D^i−C$_6$−D^i)** (≙**VII$_1$**), **4d(T^n)$_4$(D^i−C$_6$−D^i)** (≙**VIII$_1$**), and **4e(T^n)$_4$(D^i−C$_6$−D^i)** (≙**IX$_1$**) were formed after addition of equimolar amounts of the co-condensation agent **D−C$_6$−D** to the monomeric complexes (Table 1). In the case of **IX$_1$**, even under that mild reaction condition, a partial decomposition of the ruthenium(II) center was observed.

In scanning electron micrographs, the morphology of the polymers was found to be nonuniform and independent of both chemical composition and degree of condensation. Additionally, the porosity is low, which is in line with the low specific surface of these materials determined by BET measurements (Experimental Section).

Solid-State NMR Spectroscopic Characterization of the Polymer Matrixes. Owing to the amorphous nature of the polysiloxane-bound materials, solid-state NMR spectroscopy is the most important method for a structural elucidation.[36−38] A variety of different NMR spectroscopically active nuclei allow the characterization of different regions of the stationary phases presented herein. ^{29}Si NMR spectroscopy enables the investigation of the carrier matrix, the degree of condensation, and a realistic stoichiometric composition of the polymers. ^{13}C NMR describes the hydrocarbon regions of the backbone, and ^{31}P NMR offers direct access to the reactive centers.

^{29}Si CP/MAS NMR Spectroscopy. The ^{29}Si CP/MAS NMR spectra reveal signals of various substructures of the corresponding D^i and T^n functions as the result of an incomplete condensation. The average chemical

(36) Fyfe, C. A. *Solid State NMR for Chemists*; CRC Press: Gulph, ON, 1984.
(37) Engelhardt, G.; Michel, D. *High-Resolution NMR of Silicates and Zeolites*; J. Wiley & Sons: Chichester, New York, Brisbane, Toronto, Singapore, 1987; p 106.
(38) Schmidt-Rohr, K.; Spiess, H. W. *Multidimensional Solid State NMR and Polymers*; Academic Press: London, 1994.

Scheme 3

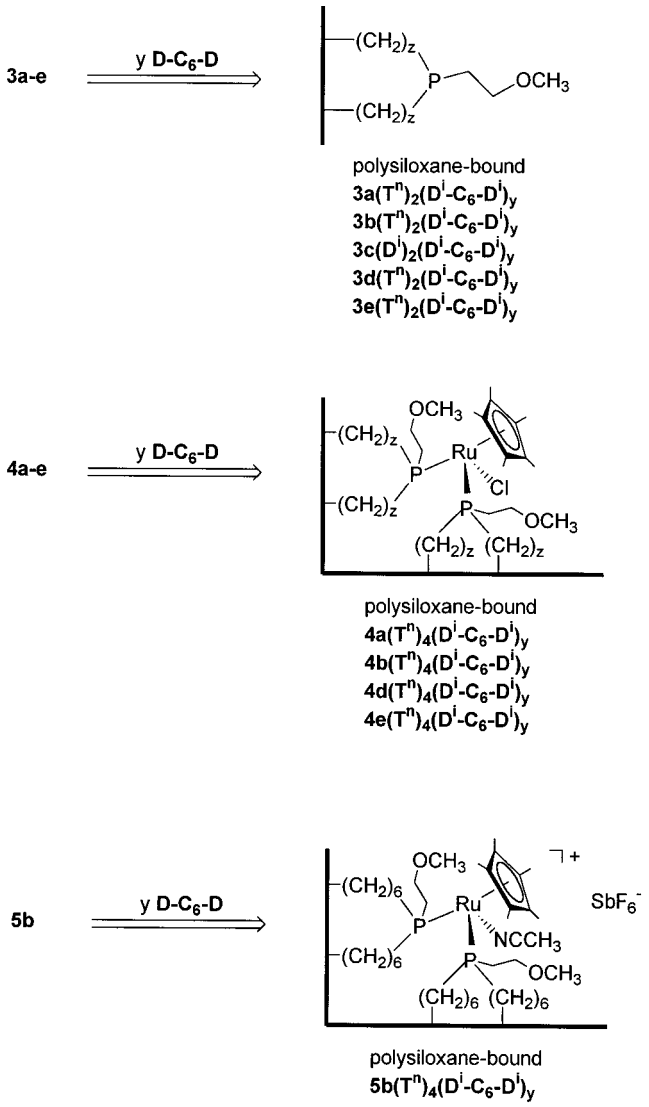

shifts[39] are −2.2 (D^0), −13.6 (D^1), −22.4 (D^2), −52.3 (T^1), −60.3 (T^2), and −68.3 (T^3). They remain unchanged with respect to the ratio between the co-condensation agent and the functionalized monomeric phosphine and complex, respectively. Since all silicon atoms of the polysiloxane matrix are in the vicinity of protons, which give rise to a sufficient Hartmann−Hahn match,[40] all silicon species are detected by ^{29}Si CP/MAS NMR spectroscopy. The degree of condensation of D and T species[41] and realistic T/D ratios are determined by generally known methods.[42]

(39) Williams, E. A. NMR Spectroscopy of Organosilicon Compounds. In *Chemistry of Organic Silicon Compounds*; Patai, S., Rappoport, Z., Eds.; J. Wiley & Sons: Chichester, New York, Brisbane, Toronto, Singapore, 1989.

(40) Maciel, G. E.; Sindorf, D. W. *J. Am. Chem. Soc.* **1980**, *102*, 7607.

(41) The degree of condensation of the T species, $100(T^1 + 2T^2 + 3T^3)/[3(T^1 + T^2 + T^3)]$; degree of condensation of the D species, $100(D^1 + 2D^2)/[2(D^0 + D^1 + D^2)]$; T^1, T^2, T^3, D^0, D^1, D^2 are the relative amounts of silyl species present in the sample (Table 2).

(42) Harris, R. K. *Analyst* **1985**, *110*, 649.

Table 1. Labeling of the Copolymers

monomeric complex	spacer length[a]	co-condensate	abbrev[b]
		(a) Co-condensed Ligands	
3a(T⁰)	3	**3a(T^n)$_2$(D^i−C$_6$−D^i)**[c]	**I$_1$**
3b(T⁰)	6	**3b(T^n)$_2$**	**II$_0$**
		3b(T^n)$_2$(D^i−C$_6$−D^i)	**II$_1$**
		3b(T^n)$_2$(D^i−C$_6$−D^i)$_2$	**II$_2$**
		3b(T^n)$_2$(D^i−C$_6$−D^i)$_4$	**II$_4$**
3c(D°)	6	**3c(D^i)$_2$(D^i−C$_6$−D^i)$_4$**	**III$_4$**
3d(T⁰)	8	**3d(T^n)$_2$(D^i−C$_6$−D^i)**	**IV$_1$**
3e(T⁰)	14	**3e(T^n)$_2$(D^i−C$_6$−D^i)**	**V$_1$**
		(b) Co-condensed Complexes	
4a(T⁰)	3	**4a(T^n)$_4$(D^i−C$_6$−D^i)**	**VI$_1$**
4b(T⁰)	6	**4b(T^n)$_4$**	**VII$_0$**
		4b(T^n)$_4$(D^i−C$_6$−D^i)	**VII$_1$**
4d(T⁰)	8	**4d(T^n)$_4$(D^i−C$_6$−D^i)**	**VIII$_1$**
4e(T⁰)	14	**4e(T^n)$_4$(D^i−C$_6$−D^i)**	**IX$_1$**
5b(T⁰)	6	**5b(T^n)$_4$(D^i−C$_6$−D^i)$_4$**	**X$_4$**

[a] Number of methylene groups between phosphorus and silicon. [b] Simplified labeling of the polymers: roman numeral, type of ligand or complex; subscript, amount of co-condensate. [c] Complete labeling of the compounds. Integer: type of reactive center; ligand (**3**), complex (**4**). Small letter: type of spacer; *n*-propyl (**a**), *n*-hexyl (**b**,**c**), *n*-octyl (**d**), *n*-tetradecyl (**e**). Capital letter: type of silicon species; three oxygen bonds (**T**), two oxygen bonds (**D**). Subscript: stoichiometry of the silicon species. Superscript: number of Si−O−Si bonds.

In former investigations, the co-condensation agent **D**−**C$_6$**−**D** demonstrated its ability to create highly cross-linked polysiloxane networks comparable to those materials which were obtained by the sol−gel processing of Si(OEt)$_4$ with Fn−T groups.[43] Therefore, the system **D**−**C$_6$**−**D**[14] (Scheme 2) was used in this investigation to compensate mobility losses caused by the application of two spacer units in the phosphines **3a,b,d,e(T⁰)** and **3c(D⁰)**. ^{29}Si CP/MAS NMR experiments of the polymers **I$_1$**−**V$_1$** reveal high degrees of condensation ranging from 85% to 97% (see Table 2). Consequently, none of the spectra show signals for D^0 or T^1 moieties. Generally, D groups in **D**−**C$_6$**−**D** polymers are better cross-linked (90−97%) than are T groups in phosphine ligands (85−91%).

High degrees of condensation are not achieved if the ruthenium(II) complexes **4a,b,d,e(T⁰)** are sol−gel processed. This is manifested in the ^{29}Si CP/MAS NMR spectra of the polymers **VI$_1$**−**X$_4$** (Figure 1), which reveal signals of D^0 and even T^0 groups (**VI$_1$, VII$_1$**). However, those D^0 and T^0 species that are attached to the polymer network via the second silyl function of the monomeric ruthenium(II) complexes or the co-condensation agent (Scheme 2) cannot be removed during the solvent processing . The higher amounts of unhydrolyzed SiOMe groups in those polymers are attributed to the reduced temperature at which the sol−gel process was performed. Consequently, for the materials **VI$_1$**−**X$_4$**, the degrees of condensation range from 52% to 99%. The cross-linking of the polymers increases with longer alkyl spacers (**VI$_1$, VII$_1$, VIII$_1$, IX$_1$**). This observation is in good agreement with former results, which showed that C_{14} spacers account for nearly quantitative condensations owing to their high flexibility.[14]

Experimentally determined stoichiometries of the copolymers **VI$_1$**−**X$_4$** differ significantly from the applied stoichiometries (Tables 1 and 2). Obviously, some of the D groups were washed out during the sol−gel process. A similar phenomenon was observed in earlier studies

Scheme 4

Idealized Composition:

$Fn[Si(OMe)_3]_2$ + y $MeSi(OMe)_2(CH_2)_6(MeO)_2SiMe$ $\xrightarrow[-\ (6+4y)\ MeOH]{+\ (3+2y)\ H_2O}$ $[Fn(SiO_{3/2})_2][MeSiO_{2/2}(CH_2)_6O_{2/2}SiMe]_y$

3(a,b,d,e) (T^0)
4 (a,b,d,e) (T^0)
5b (T^0)

3(a,b,d,e)(T^3)$_2$(D^2-C_6-D^2)$_y$
4(a,b,d,e)(T^3)$_4$(D^2-C_6-D^2)$_y$
5b(T^3)$_4$(D^2-C_6-D^2)$_y$

Realistic Composition: $\{Fn[SiO_{n/2}(OX)_{3-n}]_2\}\{MeSiO_{i/2}(OX)_{2-i}(CH_2)_6(XO)_{2-i}O_{i/2}SiMe\}_y$

3(a,b,d,e)(T^n)$_2$(D^i-C_6-D^i)$_y$
4(a,b,d,e)(T^n)$_4$(D^i-C_6-D^i)$_y$
5b(T^n)(D^i-C_6-D^i)$_y$

Idealized Composition:

$Fn[Si(OMe)_2Me]_2$ + y $MeSi(OMe)_2(CH_2)_6(MeO)_2SiMe$ $\xrightarrow[-\ (4+4y)\ MeOH]{+\ (2+2y)\ H_2O}$ $[Fn(SiO_{2/2}Me)_2][MeSiO_{2/2}(CH_2)_6O_{2/2}SiMe]_y$

3c(D^0)

3c(D^2)$_2$(D^2-C_6-D^2)$_y$

Realistic Composition: $\{Fn[SiO_{i/2}(OX)_{2-i}Me]_2\}\{MeSiO_{i/2}(OX)_{2-i}(CH_2)_6(XO)_{2-i}O_{i/2}SiMe\}_y$

3c(D^i)$_2$(D^i-C_6-D^i)$_y$

Fn= $P(CH_2CH_2OMe)[(CH_2)_z\text{-}]_2$ [**3a,b,d,e(T^0)**; **3c(D^0)**]
Fn= $[Cp^*RuCl]_{1/2}P(CH_2CH_2OMe)[(CH_2)_z\text{-}]_2$ [**4a,b,d,e(T^0)**]
Fn= $\{[Cp^*Ru(NCCH_3)]^+SbF_6^-\}_{1/2}P(CH_2CH_2OMe)[(CH_2)_z\text{-}]_2$ [**5b(T^0)**]
T = T type silicon atom (three oxygen neighbors)
D = D type silicon atom (two oxygen neighbors)
n,i = number of Si-O-Si bonds (n = 0-3; i = 0-2)
X = H, Me
y = amount of co-condensate
z = length of the $-CH_2-$ chain [z = 3, 6, 8, 14]

on polymerized ruthenium complexes in which the phosphine ligands were provided with just one spacer unit.[20] In the case of the materials **VI_1** and **X_1**, the differences are so remarkable that only qualitative comparisons of the ^{29}Si NMR spectroscopic relaxation data are reasonable.

^{13}C CP/MAS NMR Spectroscopy. All ^{13}C CP/MAS NMR spectra of the polymerized ligands (**I_1**−**V_1**) and of the ruthenium(II) complexes (**VI_1**−**X_4**) are characterized by resonances in the alkyl region between 22 and 33 ppm. In the case of the polymers prepared without any co-condensation agent (**II_0**, **VII_0**), a signal around 14 ppm indicates the methylene group adjacent to the silyl function. Another peak around 50 ppm, due to unhydrolyzed SiOMe groups, is small in the spectra of polymers with high degrees of condensation (phosphines **I_1**, **II_1**−**II_4**, **III_4**, **IV_1**, **V_1**, and complexes **IX_1** and **X_4**, Figure 2). In all other cases, a broad resonance is observed at this chemical shift. The ether function of the phosphine ligand in **II_4** gives rise to two signals at 58 and 67 ppm, which are in good agreement with the corresponding signals of its monomeric congener **3b(T^0)**. Finally, the methyl group of the D-fragment in the co-condensation agent **D**−**C_6**−**D** or in polymers derived from the monomeric precursor **3c(D^0)** resonates at 0.3 ppm. In the ^{13}C CP/MAS NMR spectra of the polymerized complexes **VI_1**−**X_4**, two additional signals at 87 and 11 ppm emphasize the existence of the C_5Me_5 fragment, and in the case of **X_4**, even the methyl group of the acetonitrile ligand is detected at 3.5 ppm (Figure 2). Additionally, a peak at −5.6 ppm points to SiMe substituents of completely unhydrolyzed D^0 species of the **D^i**−**C_6**−**D^i** material. In Figure 2, the spectra of **II_4** and **X_4** exemplarily give evidence for intact silicon−carbon and phosphorus−carbon bonds of the co-condensates, ligands, and complexes.

^{31}P CP/MAS NMR and IR Spectroscopic Characterization of the Reactive Centers. To investigate whether

Table 2. Relative I_0, T_{SiH}, and $T_{1\rho H}$ Data of the Silyl Species in the Fn−T(D)/D−C_6−D Copolymers

	relative I_0 data of D and T species[a]						degree of condensation [%]		real T/D moiety	T_{SiH} [ms][b]						$T_{1\rho H}$ [ms][c]
compd	D^0	D^1	D^2	T^1	T^2	T^3	D	T		D^0	D^1	D^2	T^1	T^2	T^3	
I_1	*d*	24.6	100.0	*d*	33.3	49.3	90.2	87.3	0.64	*e*	2.09	1.24	*e*	1.08	1.26	7.1
II_0				*d*	89.5	100.0		76.4					*e*	1.00	1.30	4.8
II_1	2.7	14.6	100.0	*d*	38.9	56.3	91.4	86.4	0.81	2.36	1.01	1.09	*e*	1.20	1.35	6.8
II_2	*d*	9.5	100.0	*d*	10.1	27.6	95.7	91.0	0.34	*e*	0.83	1.22	*e*	1.09	1.58	10.9
II_4	*d*	7.9	100.0	*d*	6.4	17.3	96.8	91.4	0.23	*e*	0.82	1.26	*e*	1.28	1.42	14.6
III_4	9.3	10.1	100.0				88.0			1.11	1.33	2.05				5.6
IV_1	*d*	16.1	100.0	*d*	48.7	68.0	93.0	86.1	1.00	*e*	2.52	1.14		1.21	1.48	5.4
V_1	*d*	8.7	100.0	*d*	31.9	43.1	96.0	85.1	0.69	*e*	0.60	1.13		1.00	1.23	8.1
VI_1	27.7	39.8	31.8	55.6	100.0	51.0	52.1	65.9	2.08	2.92	1.91	1.30	1.72	1.58	1.74	6.6
VII_0				*d*	100.0	88.2		82.3					*e*	0.92	1.22	4.64
VII_1	50.8	27.7	69.2	35.6	100.0	91.0	56.2	74.8	1.53	2.26	1.13	1.33	1.02	1.21	1.36	6.3
$VIII_1$	19.1	*d*	67.8	50.5	100.0	85.1	78.0	71.6	2.71	1.99	*e*	1.16	1.22	1.17	1.28	5.2
IX_1	*d*	*d*	100.0	*d*	77.1	56.1	100	80.7	1.33	*e*	*e*	1.18	*e*	1.32	1.09	5.5
X_4	24.0	15.5	100.0	*d*	25.8	38.1	96.0	85.8	0.46	2.24	0.99	1.20	*e*	1.20	1.29	9.4

[a] I_0 values calculated according to literature methods.[20,57] [b] Determined by contact time variation. [c] Determined via ^{29}Si with the experiment according to Schaefer (see Experimental Section). [d] Species not detectable. [e] Intensity too low for a precise determination of T_{SiH}.

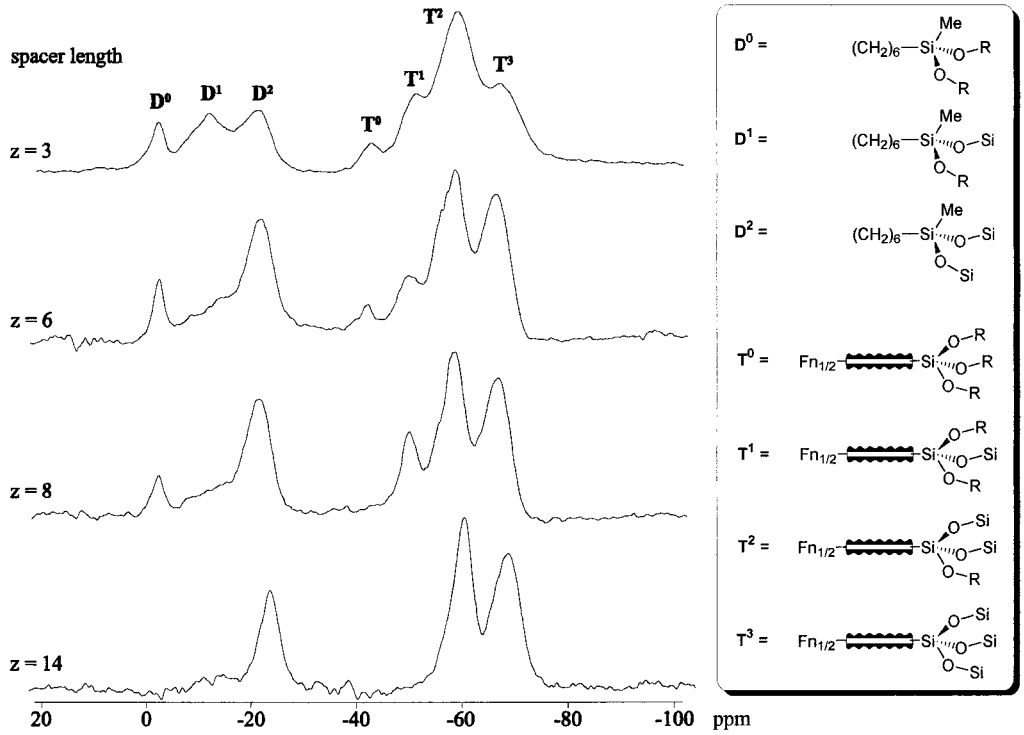

Figure 1. ^{29}Si CP/MAS NMR spectra of the copolymers **VI_1**, **VII_1**, **$VIII_1$**, and **IX_1**. The various silyl species are displayed schematically.

the phosphine ligand or complex fragments remain intact during the sol−gel processing, ^{31}P CP/MAS NMR measurements have been performed. In the case of the phosphines **3a,b,d,e(T^0)** and **3c(D^0),** no decomposition during the polymerization takes place, since only one signal is detected for the polymers **I_1**−**V_1** at −35 ppm, which is compatible with the monomeric precursors **3a,b,d,e(T^0)** and **3c(D^0)**. In the spectra of the polymers **VI_1**−**IX_1**, the resonances around 14 ppm, flanked by spinning sidebands, points to the intact polymerized complex. For **X_4**, however, a signal at 15.3 ppm occurs (Table 3). In the latter case, the ruthenium center is stabilized by the coordinated acetonitrile molecule during the sol−gel process. Acetonitrile is still coordinated to ruthenium in **X_4**, which is confirmed by a C≡N absorption at 2261 cm^{-1} in the IR spectrum of dry **X_4**. This vibration is comparable to that of the monomeric congener **5b(T^0)** in solution (see Scheme 3 and Experimental Section).

EXAFS Spectroscopic Characterization of 4b-(T^n)$_4$. Since the discussed materials are of amorphous nature, the information about the atomic environment around the ruthenium center is provided by EXAFS spectroscopy, as it operates independently on the physical state of the samples. Therefore, **4b(T^n)$_4$** (≙**VII_0**) was prepared without any co-condensation agent to maintain a high content of ruthenium in the polymer.

The k^3-weighted EXAFS function (Figure 3) is described best by three different shells: the carbon atoms of the C_5Me_5 ring, the phosphorus atoms of the phosphine ligands, and the chlorine atom. As it can be derived from the Fourier transforms, all these shells give rise to only one intensive peak due to the small difference of their distances to the absorber, but their

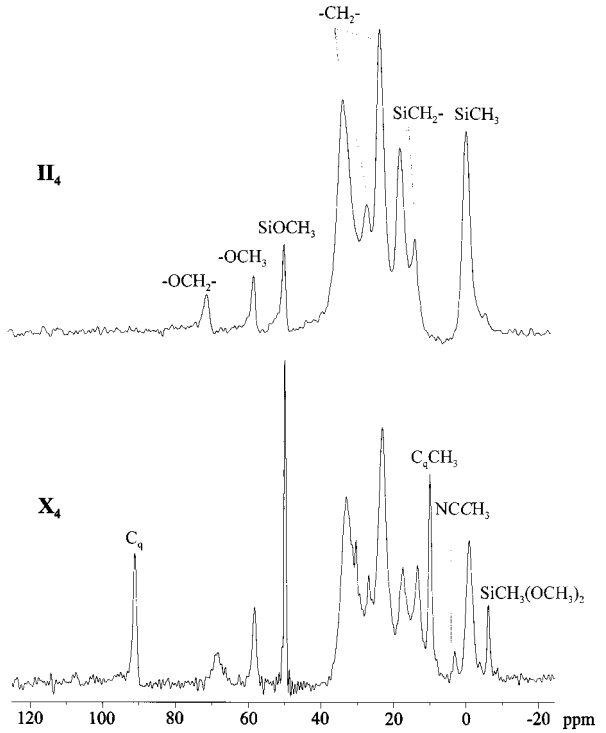

Figure 2. ^{13}C CP/MAS NMR spectra of $\mathbf{II_4}$ [polymerized phosphine ligand] and $\mathbf{X_4}$ [polymerized cationic ruthenium(II) complex] (ν_{rf} = 10 kHz).

Table 3. ^{31}P CP/MAS, T_{PH}, and $T_{1\rho H}$ Data of the Polysiloxane-Bound Ether−Phosphine Ligands I−V and the Complexes VI−X

compd	δ^{31}P [ppm]	T_{PH} [μs][a]	$T_{1\rho H}$ [ms][b]	T_{1P} [s][c]
$\mathbf{I_1}$	−36.7	262.5	7.8	3.3
$\mathbf{II_0}$	−35.5	332.1	5.8	*d*
$\mathbf{II_1}$	−35.8	360.3	10.0	2.5
$\mathbf{II_2}$	−35.5	406.9	9.8	*d*
$\mathbf{II_4}$	−35.5	414.9	8.9	*d*
$\mathbf{III_4}$	−35.5	731.3	3.5	*d*
$\mathbf{IV_1}$	−36.0	1360.0	2.0	2.4
$\mathbf{V_1}$	−35.8	1230.0	3.4	1.8
$\mathbf{VI_1}$	14.1	153.2	5.2	*d*
$\mathbf{VII_0}$	14.7	334.7	*d*	*d*
$\mathbf{VII_1}$	14.5	163.0	6.6	*d*
$\mathbf{VIII_1}$	14.5	148.0	5.4	*d*
$\mathbf{IX_1}$	14.5	159.2	5.3	*d*
$\mathbf{X_4}$	15.3	217.1	11.1	*d*

[a] Determined by contact time variation. [b] Determined by ^{31}P with the experiment according to Schaefer (see Experimental Section). [c] Values from the NMR experiment according to Torchia (see Experimental Section) at 294 K. [d] Values not determined.

contribution to the EXAFS function is significant. The determined ruthenium−chlorine bond distance (Table 4) is in good agreement with literature data of comparable (η^5-C_5Me_5)chlororuthenium(II) complexes obtained by X-ray diffraction studies.[44] The average values for the ruthenium−phosphorus bonds (237 pm) and the ruthenium−carbon bonds (227 pm) were found to be slightly longer than literature results.[45]

Studies on the Dynamic Behavior of the Polysiloxanes by ^{29}Si,^{31}P CP/MAS NMR and 2D-WISE

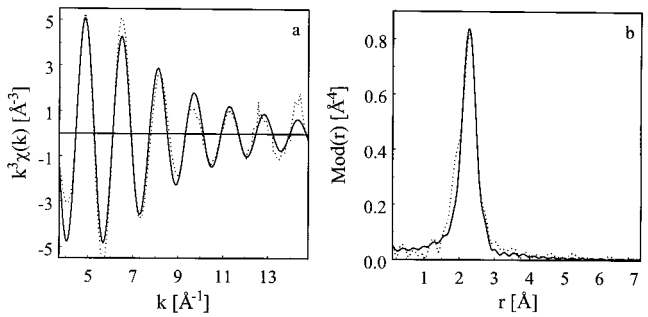

Figure 3. Calculated (solid line) and experimental (dotted line) $k^3\chi(k)$ function (a) and their Fourier transforms (b) (Ru−K-edge) in the k-range 3−14.6 Å^{-1}.

Table 4. EXAFS Spectroscopically Determined Structural Data, Absorber−Backscatterer Distance, Coordination Number, and Debye−Waller Factor (σ) of $\mathbf{VII_0}$ (Errors of r and σ Given in Parentheses), Energy Shift ΔE_0 = 19.8 ±0.62 eV

	r [Å]	N[a]	σ [Å]
Ru−C	2.27 (±0.02)	5	0.120 (±0.008)
Ru−P	2.37 (±0.02)	2	0.074 (±0.004)
Ru−Cl	2.46 (±0.03)	1	0.089 (±0.005)

[a] See Experimental Section.

NMR Spectroscopy. Detailed knowledge of the dynamic properties of the different parts of a stationary phase is necessary for its optimization in interphases. Enhancing mobilities should account for higher flexibility, accessibility, and uniformity of the reactive centers and thus for higher activities and selectivities in catalytic reactions. As shown in recent investigations, several NMR parameters, e.g., relaxation and cross-polarization parameters are sensitive toward motions.[14,38,43]

Mobility of the Matrix. The $T_{1\rho H}$ data extracted from ^{29}Si CP/MAS NMR measurements of the copolymerized ligands $\mathbf{I_1}$−$\mathbf{V_1}$ depend on the spacer length as well as on the amount of the co-condensation agent $\mathbf{D}$−$\mathbf{C_6}$−$\mathbf{D}$ (Table 2). Longer $T_{1\rho H}$ values were recorded for higher amounts of the co-condensation agent, thus indicating an increasing mobility. As expected, two spacer units per ligand give rise to a reduced flexibility of the polymers compared to phosphines with just one spacer.[20] In contrast to the $T_{1\rho H}$ data of the ligands $\mathbf{I_1}$−$\mathbf{V_1}$, the corresponding values for the hybrid polymers $\mathbf{VI_1}$−$\mathbf{IX_1}$ are in good agreement with results previously reported.[8]

Mobility of the Reactive Center. Phosphorus atoms are an excellent probe to study the influence on the mobility of different spacer lengths, amounts of co-condensates, and other changes within the stationary phases. With an increasing spacer length, the mobility is enhanced, with $\mathbf{V_1}$ being even in the fast motion regime of the correlation time curve, as is demonstrated by temperature-dependent measurements of $T_{1\rho H}$ and T_{1P} (Figures 4 and 5). Additionally, a decrease of the T_{1P} relaxation time further confirms a mobility enhancement on going from an *n*-propyl to an *n*-tetradecyl spacer, which agrees with the reduction of the line width (Figure 6).

The amount of the co-condensation agent $\mathbf{D}$−$\mathbf{C_6}$−$\mathbf{D}$ (Scheme 2) does not influence the mobility significantly. Compared to polymers without $\mathbf{D}$−$\mathbf{C_6}$−$\mathbf{D}$ ($\mathbf{II_0}$, $\mathbf{VII_0}$), the presence of this co-condensate generally leads to an increase in mobility, however, this effect is not improved by variation of the amount of $\mathbf{D}$−$\mathbf{C_6}$−$\mathbf{D}$.

(43) Lindner, E.; Kemmler, M.; Mayer, H. A.; Wegner, P. *J. Am. Chem. Soc.* **1994**, *116*, 348.
(44) Lubián, R. T.; Paz-Sandoval, M. A. *J. Organomet. Chem.* **1997**, *532*, 17.
(45) De los Ríos, I.; Tenorio, M. J.; Padilla, J.; Puerta, M. C.; Valerga, P. *J. Chem. Soc., Dalton Trans.* **1996**, 377.

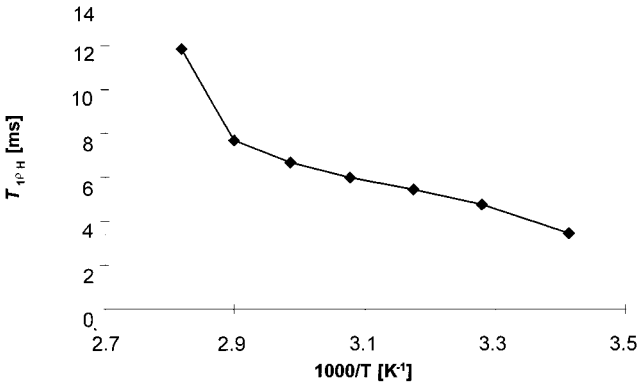

Figure 4. Plot of $T_{1\rho H}$ versus temperature of **III$_4$**.

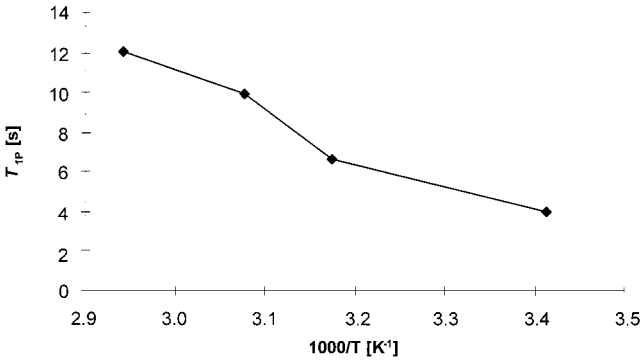

Figure 5. Temperature-dependent T_{1P} relaxation measurement of **V$_1$**.

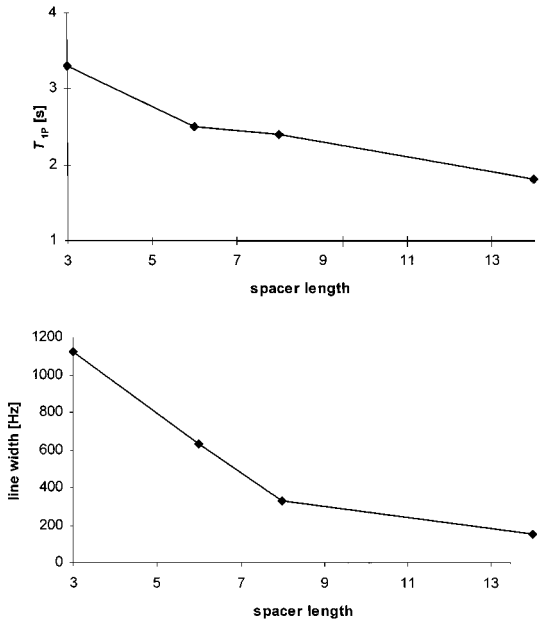

Figure 6. Relaxation rate T_{1P} and line width as a function of the *n*-alkyl spacer lengths of **I$_1$**, **II$_1$**, **IV$_1$**, and **V$_1$**.

Further increase in the mobility should be expected by replacing the T-silyl function of the ligands by a D group, reducing the number of Si−O−Si bonds and thus generating more flexibility. This is supported by a significantly higher cross-polarization constant T_{PH} and a lower relaxation rate constant $T_{1\rho H}$ obtained for ligand **III$_4$**. As already observed for the T analogues, the effect of increasing amounts of **D−C$_6$−D** is rather low. The ruthenium(II) complexes with T-functionalized ligands show no significant mobility enhancement, since neither $T_{1\rho H}$ nor T_{PH} vary with increasing spacer length, which indicates the rigid influence of the two spacer units per phosphine ligand.

2D-WISE Experiments. 2D-WISE experiments enable a direct correlation between the segmental mobility and the structural information in order to gain a more detailed insight into the dynamic behavior of inorganic−organic hybrid materials.[38] 2D spectra show structural information along the one axis and mobilities along the other axis. Slices along a certain chemical shift give access to the corresponding line width of the various moieties within a sample. The line widths in the F1 (proton) dimension are determined by ^{1}H−^{1}H dipolar interactions, which are reduced by molecular motion and magic-angle spinning. ^{13}C 2D-WISE spectra were recorded for the complex **X$_4$** in the solid state (Figure 7) and in the interphase (Figure 8). The high rigidity caused by the two spacer units is confirmed by broad lines in the proton dimension. After the hybrid system is swollen with ethanol, the mobility is enhanced; however, the line widths of 2D spectra of previously reported catalysts[46] show a stronger reduction after treatment of the inorganic−organic hybrid material with solvents. These findings agree well with results obtained by relaxation time measurements. The increase of rigidity caused by two spacer units attached to only one phosphorus atom is hard to compensate.

Conclusion

One of the most aggravating problems arising from the combination of the advantages of homogeneous and heterogeneous catalysts is the leaching of the catalytically active centers from the polymeric support. To overcome this serious obstacle, several approaches have been reported in the literature.[4,5,17] In this investigation, the hemilabile ether phosphine ligands **3a,b,d,e(T^0)** and **3c(D^0)** are provided with T- and D-functionalized spacer units. The sol−gel process of these ligands leads to the highly cross-linked stationary phases **I$_1$**−**V$_1$** (Table 1). Relaxation times ($T_{1\rho H}$) and cross-polarization parameters (T_{PH}, T_{SiH}), which are obtained from solid-state NMR experiments, point to reduced mobilities of these materials similar to the case for polymers containing Q groups.[43] This impairment of flexibility is increased if ligands are coordinated to transition metal complexes.[14,20,43] In the case of the polymeric ruthenium(II) complexes **VI$_1$**−**X$_4$** (Table 1), which are accessible from the soluble precursor complexes **4a,b,d,e(T^0)**, the anchoring via four spacers and the mentioned effect of complexation affect the mobility of the reactive centers considerably. Whereas the incorporation of longer alkyl spacers and of the co-condensation agent **D−C$_6$−D** (Scheme 2) largely compensates for the mobility loss of the polycondensed ligands **I$_1$**−**V$_1$**, in the case of the corresponding ruthenium(II) complexes **VI$_1$**−**X$_4$**, the materials remain rigid.

With the example of the (η^5-C$_5$Me$_5$)chlororuthenium(II) complex **4b(T^0)** it was demonstrated that it is a valuable educt for the synthesis of a cationic congener which should be able to activate catalytically relevant small molecules.[22,45] The abstraction of Cl$^-$ is successful

(46) Lindner, E.; Auer, F.; Baumann, A.; Wegner, P.; Mayer, H. A.; Bertagnolli, H.; Reinöhl, U.; Ertel, T. S.; Weber, A. *J. Mol. Catal.*, submitted for publication.

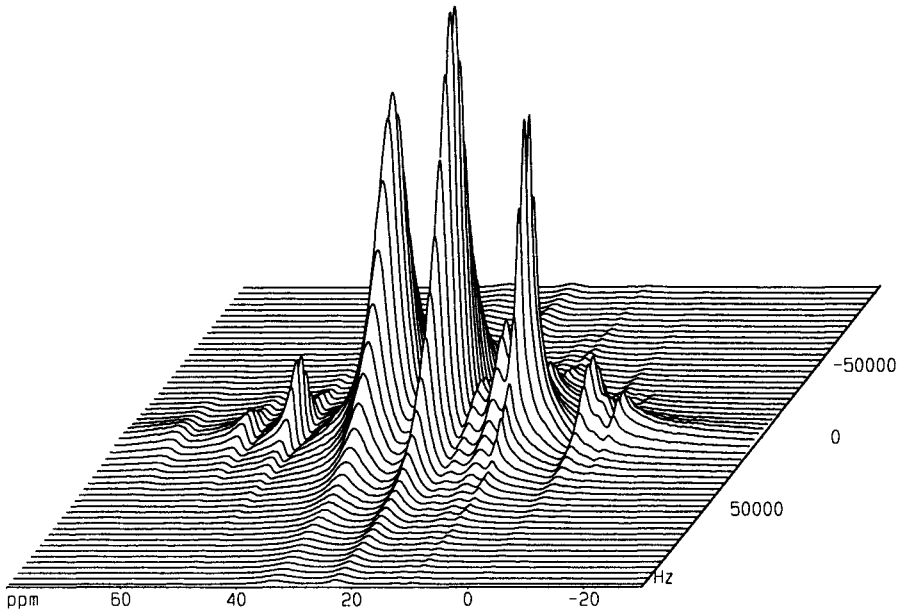

Figure 7. $^{1}H,^{13}C$ 2D-WISE spectrum of $\mathbf{X_4}$ in the dry state.

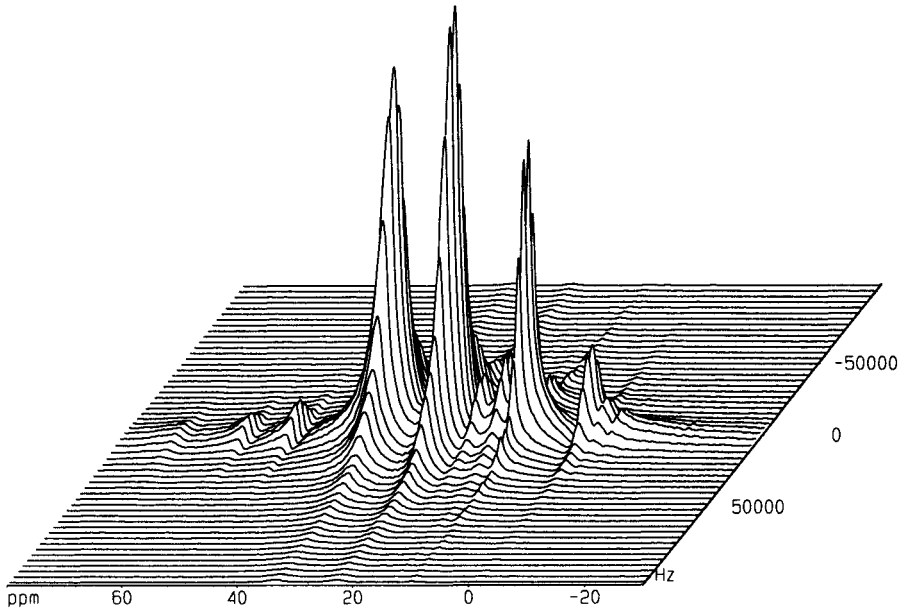

Figure 8. $^{1}H,^{13}C$ 2D-WISE spectrum of $\mathbf{X_4}$ swollen in EtOH.

with $AgSbF_6$, and the empty coordination site is protected by an intramolecular ether oxygen donor. Ruthenium complexes containing O∩P chelates have gained interest as catalysts in ring opening metatheses (ROMP).[47] However, from previous experiences it is known that ether phosphine chelates of transition metals do not survive the sol−gel process.[8] A successful alternative is offered by introduction of an easily removable solvent as a ligand.[8,15] In the present case, acetonitrile was employed and **4b(T⁰)** was transferred to the cationic acetonitrile complex **5b(T⁰)**. The latter was subjected to a polycondensation in the presence of the co-condensation agent **D**−$\mathbf{C_6}$−**D** (Scheme 2) to give the polymeric cationic complex $\mathbf{X_4}$ (Table 1).

2D-WISE NMR investigations on the stationary phase $\mathbf{X_4}$ and the interphase $\mathbf{X_4}$ + EtOH reveal that the high rigidity of this material is noticably eliminated in an interphase. This observation is confirmed by the reaction of $\mathbf{X_4}$ in toluene with carbon monoxide resulting in the formation of a carbonyl complex.[48]

Experimental Section

Elemental analyses were carried out on a Carlo Erba model 1106 analyzer; Cl analyses were performed according to Dirschel and Erne[49] and Schöniger.[50] Solution nuclear magnetic resonance spectra (NMR) were recorded on a Bruker DRX 250 spectrometer at 298 K. Frequencies and standards were as follows: $^{31}P\{^{1}H\}$ NMR, 101.25 MHz; $^{13}C\{^{1}H\}$ NMR, 62.90 MHz; ^{1}H NMR, 250.13 MHz. All NMR spectra were calibrated relative to partially deuterated solvent peaks which are reported relative to tetramethylsilane (TMS). Mass spectra

(47) Lindner, E.; Pautz, S.; Fawzi, R.; Steimann, M. *Organometallics* **1998**, *17*, 3006.

(48) Wielandt, W. Ph.D. Thesis, University of Tübingen, 1999.
(49) Dirschel, A.; Erne, F. *Microchim. Acta* **1961**, 866.
(50) (a) Schöniger, W. *Microchim. Acta* **1955**, 123. (b) Schöniger, W. *Microchim. Acta* **1956**, 869.

were acquired on a Finnigan TSQ 70 instrument [electron ionization], on a Finnigan MAT 711A instrument (8kV, 333K) modified by AMD (Harpstedt, Germany) [field desorption], or on a Finnigan MAT TSQ 70 (10 kV, 50 °C) [fast atom bombardement], respectively, and are reported as mass/charge (*m*/*z*).

CP/MAS solid-state NMR spectra were recorded on Bruker MSL and DSX 200 (4.7 T) multinuclear spectrometers (^{29}Si) and a Bruker ASX 300 (7.05 T) spectrometer (^{13}C and ^{31}P) equipped with wide-bore magnets. Magic-angle spinning was applied at 3 kHz (^{29}Si) or 10−12 kHz (^{13}C, ^{31}P). All samples were packed under exclusion of molecular oxygen. Frequencies and standards: ^{31}P, 121.49 MHz [85% H_3PO_4, $NH_4H_2PO_4$ as second standard]; ^{13}C, 50.325 MHz [TMS, carbonyl resonance of glycine (δ = 170.09 ppm) as second standard]; ^{29}Si, 39.75 MHz (Q_8M_8). The cross-polarization constants T_{PH} and T_{SiH} were determined by variations of the contact time (20−25 experiments). The proton relaxation time in the rotating frame $T_{1\rho H}$ was measured by direct proton spin lock-τ-CP experiments as described by Schaefer and Stejskal.[51] T_{1P} values were received using the method developed by Torchia.[52] The relaxation time data were obtained by using the Bruker software SIMFIT or Jandel software PEAKFIT. Peak deconvolution of the spectra was performed with the Bruker-Spectrospin software XNMR using Voigtian line shapes. The WISE NMR spectra were recorded under MAS conditions (3 kHz). 64 t_1 increments with a dwelling time of 3−10 μs were used for each spectrum. Cross polarization was applied with contact times of 200 μs for WISE experiments to eliminate spin-diffusion effects and of 2−5 ms for CP/MAS experiments, respectively.

The EXAFS measurements of **4b(T^n)$_4$** were performed at the ruthenium K-edge (22118 eV) at the beamline A1 of the Hamburger Synchrotronstrahlungslabor (HASYLAB) at DESY, Hamburg, under ambient conditions, positron energy 4.5 GeV, and initial beam current 120 mA. For harmonic rejection, the second crystal of the Si(311) double crystal monochromator was tilted to 30%. Data were collected in transmission mode with the ion chambers flushed with argon. The energy was calibrated with a ruthenium metal foil of 20 μm thickness. The sample itself was prepared by pressing a mixture of 240 mg of **4b(T^n)$_4$** and 40 mg polyethylene into a tablet of 1.3 cm diameter and 0.2 cm thickness.

The data were analyzed with a program package developed for the investigation of amorphous solids.[53] Background subtraction was done with AUTOBK from the University of Washington,[54] the evaluation in k-space was performed with the EXCURV92 module[55] xalpha potentials and phaseshifts of the program package CERIUS2. The amplitude reduction factor AFAC was set to 0.8, and an overall energy shift E_f was introduced to obtain the best fit to the data. The coordination numbers of the backscatterers were fixed at the known values in order to reduce the number of independent parameters.

The surface areas were determined by analyzing the N_2 adsorption isotherms according to the BET method using a Micromeritics Gemini. All manipulations were performed under an atmosphere of argon by employing usual Schlenk techniques. All solvents were dried according to common methods, distilled, and stored under argon. The silyl compounds **2a**−**e**,[48] the co-condensation agent **D**−**C$_6$**−**D**,[20] $H_3COCH_2CH_2P(O)(OEt)_2$,[56] and $[Cp^*RuCl]_4$[29] were synthesized according to literature methods. $LiAlH_4$ and $(n\text{-}Bu)_2Sn(OAc)_2$ were purchased from Merck (Darmstadt, Germany) and stored under argon.

2-Methoxyethylphosphine (1). Diethyl(2-methoxyethyl)-phosphonate (21.1 g, 107.6 mmol) was added dropwise to a suspension of 4.8 g (126.3 mmol) of $LiAlH_4$ in 100 mL of di-*n*-butyl ether at 0 °C. The mixture was warmed to room temperature and stirred for 2 h. The crude product was distilled, bp 75 °C: yield 3.96 g (40%); ^{31}P NMR ($CDCl_3$) δ −152.65 (mt, $^1J_{PH}$ = 194 Hz, $^2J_{PH}$ = 5.1 Hz); ^{13}C{^{1}H} NMR ($CDCl_3$) δ 75.1 (s, $PCH_2CH_2OCH_3$), 58.7 (s, OCH_3), 15.0 (d, $^1J_{PC}$ = 10.1 Hz, $PCH_2CH_2OCH_3$); ^{1}H NMR ($CDCl_3$) δ 3.25 (m, 2H, $PCH_2CH_2OCH_3$), 3.09 (s, 3H, OCH_3), 2.37 (dt, $^1J_{PH}$ = 194 Hz, $^3J_{HH}$ = 5.1 Hz, 2H, H_2PCH_2), 1.52 (m, 2H, PCH_2).

Synthesis of the Monomeric Phosphines 3a,b,d,e(T^0) and 3c(D^0). A mixture of **1** and a double molar ratio of the corresponding silane **2a**−**e** was exposed to UV light and stirred for 16 h. The course of the reaction was controlled ^{31}P NMR spectroscopically. After the reaction had finished, the crude product was concentrated in vacuo to remove di-*n*-butyl ether and excess silane. The yields varied between 60% and 90%.

(2-Methoxyethyl)bis[(3-trimethoxysilyl)propyl]phosphine [3a(T^0)]. **1** (4.00 g, 43.442 mmol) was reacted with **2a(T^0)** (14.10 g, 86.897 mmol) by exposure to UV light for 16 h: yield 14.2 g (78.6%); ^{31}P{^{1}H} NMR ($CDCl_3$) δ −35.96 (s); ^{13}C{^{1}H} NMR ($CDCl_3$) δ 70.25 (d, $^2J_{PC}$ = 20.2 Hz, $PCH_2CH_2OCH_3$), 58.05 (s, OCH_3), 50.12 (s, $SiOCH_3$), 30.71 (d, $^1J_{PC}$ = 11.5 Hz, $PCH_2CH_2CH_2Si$), 27.43 (d, $^1J_{PC}$ = 14.1 Hz, $PCH_2CH_2OCH_3$), 19.05 (d, $^2J_{PC}$ = 14.8 Hz, $PCH_2CH_2CH_2Si$), 10.94 (d, $^3J_{PC}$ = 10.8 Hz, $PCH_2CH_2CH_2Si$); ^{1}H NMR ($CDCl_3$) δ 3.50 (s, 18H, $SiOCH_3$), 3.44 (t, $^3J_{HH}$ = 7.4 Hz, 2H, $PCH_2CH_2OCH_3$), 3.27 (s, 3H, OCH_3), 1.64 (t, $^3J_{HH}$ = 7.4 Hz, 2H, $PCH_2CH_2OCH_3$), 1.44 (m, 8H, $PCH_2CH_2CH_2Si$), 0.70 (m,[58] N = 14.8 Hz, 4H, $PCH_2CH_2CH_2Si$); EI-MS *m*/*z* 416 (M^+, 10), 326 [$M^+ - OCH_3 - CH_2CH_2OCH_3$, 48], 121 [$Si(OCH_3)_3$, 100]. Anal. Calcd for $C_{15}H_{37}O_7PSi_2$: C, 43.25; H, 8.95. Found: C, 43.21; H, 8.82.

Synthesis of the Monomeric Cp*Ru(II) Complexes 4a,b,d,e(T^0). A double molar amount of the corresponding phosphines **3a,b,d,e(T^0)** in 20 mL of CH_2Cl_2 was dropped into a solution of $[Cp^*RuCl]_4$ in 20 mL of CH_2Cl_2. After stirring for 1 h, the solvent was removed completely in vacuo to yield a viscous red-brown oil (90−95%).

Chlorobis{(2-methoxyethyl)bis[(3-trimethoxysilyl)propyl]phosphine-*P*}(η^5-pentamethylcyclopentadienyl)ruthenium(II) [4a(T^0)]. $[Cp^*RuCl]_4$ (294 mg, 0.27 mmol) dissolved in 15 mL of CH_2Cl_2 was reacted with 900 mg (2.16 mmol) of **3a(T^0)** in 10 mL of CH_2Cl_2 to yield 1.15 g of **4a(T^0)** (96.4%): ^{31}P{^{1}H} NMR ($CDCl_3$) δ 14.98 (s); ^{13}C{^{1}H} NMR ($CDCl_3$) δ 86.91 (s, C_5Me_5), 68.84 (s, $PCH_2CH_2OCH_3$), 58.11 (s, OCH_3), 50.16 (s, $SiOCH_3$), 33.37, 32.22 (m,[58] N = 20.6 Hz, $PCH_2CH_2CH_2Si$), 28.31 (m,[58] N = 20.2 Hz, $PCH_2CH_2OCH_3$), 18.16, 17.75 (s, $PCH_2CH_2CH_2Si$), 11.06 (s, $PCH_2CH_2CH_2Si$), 10.12 (s, CH_3); FD-MS *m*/*z* 1104 (M^+, 100). Anal. Calcd for $C_{40}H_{89}ClO_{14}P_2RuSi_4$: C, 43.48; H, 8.12; Cl, 3.21. Found: C, 43.84; H, 8.07; Cl, 3.26.

Acetonitrilebis{(2-methoxyethyl)bis[(3-trimethoxysilyl)hexyl]phosphine-*P*}(η^5-pentamethylcyclopentadienyl)-ruthenium(II) Hexafluoroantimonate [5b(T^0)]. **4b(T^0)** (1.177 g, 0.924 mmol) dissolved in 40 mL of H_3CCN was reacted with $AgSbF_6$ (320 mg, 0.931 mmol) in 10 mL of H_3CCN to yield 1.26 g of **5b(T^0)** (90.0%): IR (KBr, cm^{-1}) ν(CN) 2259 (w); ^{31}P{^{1}H} NMR (C_6D_6) δ 17.63 (s); ^{13}C{^{1}H} NMR (C_6D_6) δ 124.28 (s, $NCCH_3$), 90.90 (s, C_5Me_5), 68.41 (s, $PCH_2CH_2OCH_3$), 58.36 (s, OCH_3), 50.28 (s, $SiOCH_3$), 32.93 (s, $CH_2CH_2CH_2Si$), 31.28 (m,[58] N = 10.8 Hz, $PCH_2CH_2CH_2$), 29.3−28.5 (m, $PCH_2CH_2OCH_3$, $PCH_2CH_2CH_2$), 24.43 (s, $PCH_2CH_2CH_2$), 23.05 (s, $CH_2CH_2CH_2Si$), 10.35 (s, CH_2Si), 9.59 (s, CH_3), 3.44 (s; $NCCH_3$); FD-MS *m*/*z* 1472.8 ($M^+ - NCCH_3$, 27), 1238.1 ($M^+ - NCCH_3 - SbF_6$, 100). Anal. Calcd for $C_{54}H_{116}F_6NO_{14}P_2RuSi_4Sb$: C, 42.82; H, 7.72; N, 0.93. Found: C, 41.52; H, 7.52; N, 1.02.

Sol−Gel Processing of the Phosphines 3 and Cp*Ru(II) Complexes 4 and 5b(T^0). The monomers **3a,b,d,e(T^0)**, **3c(D^0)**, **4a,b,d,e(T^0)**, and **5b(T^0)**, specified quantities *y* of **D^0**−**C$_6$**−**D^0** (*y* = 0, 1, 2, 4), 0.5 mL of water, and the catalyst (*n*-

(51) Schaefer, J.; Stejskal, E. O.; Buchdahl, R. *Macromolecules* **1977**, *10*, 384.
(52) Torchia, A. D. *J. Magn. Reson.* **1978**, *30*, 613.
(53) Ertel, T. S.; Bertagnolli, H.; Hueckmann, S.; Kolb, U.; Peter, D. *Appl. Spectrosc.* **1992**, *46*, 690.
(54) Newville, M.; Livins, P.; Yakobi, Y.; Rehr, J. J.; Stern, E. A. *Phys. Rev. B* **1993**, *47*, 14126.
(55) Gurman, S. J.; Binsted, N.; Ross, I. *J. Phys. C* **1986**, *19*, 1845.
(56) Pudovic, A. N.; Kuzovleva, R. G. *Zh. Obshch. Khim.* **1963**, *33*, 2755; *Chem. Abstr.* **1964**, *60*, 543b.
(57) Mehring, M. *Principles of High-Resolution NMR in Solids*, 2nd ed.; Springer-Verlag: Berlin, 1983.
(58) m: *AA'XX'* pattern.

$Bu)_2Sn(OAc)_2$ were homogenized in 5 mL of MeOH. The mixtures were sealed in a Schlenk tube and stirred for 24 h until a gel was formed. Subsequently, the solvents were removed under reduced pressure and the gels were dried for 4 h. Solvent processing was performed by vigorous stirring of the large gel particles in 25 mL of toluene (2 h), leading to sufficiently swollen gels. The wet gels were washed with 25 mL of toluene, 25 mL of MeOH, and 25 mL of *n*-hexane. The polymers gave colorless gels on sol−gel processing and white powders when dried for 16 h in vacuo. Incorporation of Ru(II)-doped precursors resulted in reddish-brown gels on sol−gel processing at −20 °C and brown powders when dried.

(2-Methoxyethyl)bis[polysiloxanylpropyl]phosphine [3a(T^n)$_2$(D^i−C_6−D^i) I_1, See Table 1]. A mixture of **3a(T^0)** (824 mg, 1.978 mmol), 1 equiv of **D^0−C_6−D^0** (634 mg, 2.153 mmol), water (0.5 mL, 27.778 mmol), and $(n\text{-Bu})_2Sn(OAc)_2$ (27 mg, 0.077 mmol) in 5 mL of MeOH was sol−gel processed: yield 945 mg (95.8%); ^{31}P CP/MAS NMR δ −37.2; ^{13}C CP/MAS NMR δ 71.6 ($PCH_2\mathit{C}H_2OCH_3$), 58.7 ($PCH_2CH_2\mathit{O}CH_3$), 50.6 ($SiOCH_3$), 33.3 [$Si(CH_2)_2\mathit{C}H_2\mathit{C}H_2(CH_2)_2Si$], 27.8 ($P\mathit{C}H_2CH_2OCH_3$), 23.7 ($PCH_2\mathit{C}H_2CH_2Si$), 18.0 [$P\mathit{C}H_2CH_2\mathit{C}H_2Si$, $Si(\mathit{C}H_2)_2CH_2CH_2(\mathit{C}H_2)_2Si$], 0.3 ($SiCH_3$); ^{29}Si CP/MAS NMR (silicon substructure) δ −2.2 (D^0), −13.9 (D^1), −22.2 (D^2), −59.4 (T^2), −68.3 (T^3). N_2 surface area: 1.43 m^2/g. Anal. Calcd for $C_{17}H_{37}O_6PSi_4$ (idealized stoichiometry): C, 42.47; H, 7.76. Corrected stoichiometry:[59] C, 43.11; H, 8.10. Found: C, 40.95; H, 7.13.

(2-Methoxyethyl)bis[polysiloxanylhexyl]phosphine [3b(T^n)$_2$ ≙ II_0]. A mixture of **3b(T^0)** (787 mg, 1.572 mmol), water (0.5 mL, 27.778 mmol), and $(n\text{-Bu})_2Sn(OAc)_2$ (27 mg, 0.077 mmol) in 5 mL of MeOH was sol−gel processed: yield 545 mg (95.6%); ^{31}P CP/MAS NMR δ −35.5; ^{13}C CP/MAS NMR δ 70.9 ($PCH_2\mathit{C}H_2OCH_3$), 58.3 ($PCH_2CH_2\mathit{O}CH_3$), 50.1 ($SiOCH_3$), 32.5 [$P(CH_2)_2\mathit{C}H_2\mathit{C}H_2(CH_2)_2Si$], 27.2 [$P\mathit{C}H_2CH_2OCH_3$, $P(\mathit{C}H_2)_2(CH_2)_4Si$], 23.6 [$P(CH_2)_4\mathit{C}H_2CH_2Si$], 13.9 [$P(CH_2)_5\mathit{C}H_2Si$]; ^{29}Si CP/MAS NMR (silicon substructure) δ −60.3 (T^2), −67.0 (T^3). N_2 surface area: 1.04 m^2/g. Anal. Calcd for $C_{15}H_{31}O_4PSi_2$ (idealized stoichiometry): C, 49.69; H, 8.62. Corrected stoichiometry:[59] C, 46.67; H, 8.41. Found: C, 45.44; H, 7.91.

(2-Methoxyethyl)bis[polysiloxanylhexyl]phosphine [3b(T^n)$_2$(D^i−C_6−D^i) ≙ II_1]. A mixture of **3b(T^0)** (454 mg, 0.907 mmol), 1 equiv of **D^0−C_6−D^0** (329 mg, 1.117 mmol), water (0.5 mL, 27.778 mmol), and $(n\text{-Bu})_2Sn(OAc)_2$ (27 mg, 0.077 mmol) in 5 mL of MeOH was sol−gel processed: yield 530 mg (95.5%); ^{31}P CP/MAS NMR δ −35.8; ^{13}C CP/MAS NMR δ 71.1 ($PCH_2\mathit{C}H_2OCH_3$), 58.2 ($PCH_2CH_2\mathit{O}CH_3$), 49.8 ($SiOCH_3$), 33.1 [$P(CH_2)_2\mathit{C}H_2\mathit{C}H_2(CH_2)_2Si$, $Si(CH_2)_2\mathit{C}H_2\mathit{C}H_2(CH_2)_2Si$], 27.1 [$P\mathit{C}H_2CH_2OCH_3$, $P(\mathit{C}H_2)_2(CH_2)_4Si$], 23.5 [$P(CH_2)_4\mathit{C}H_2CH_2Si$, $SiCH_2\mathit{C}H_2(CH_2)_2\mathit{C}H_2CH_2Si$], 17.9 [$Si\mathit{C}H_2(CH_2)_4\mathit{C}H_2Si$], 14.0 [$P(CH_2)_5\mathit{C}H_2Si$], −0.2 ($SiCH_3$); ^{29}Si CP/MAS NMR (silicon substructure) δ −2.1 (D^0), −13.8 (D^1), −22.6 (D^2), −58.8 (T^2), −67.2 (T^3). N_2 surface area: 0.97 m^2/g. Anal. Calcd for $C_{23}H_{49}O_6PSi_4$ (idealized stoichiometry): C, 48.90; H, 8.74. Corrected stoichiometry:[59] C, 48.20; H, 8.82. Found: C, 49.04; H, 8.40.

(2-Methoxyethyl)bis[polysiloxanylhexyl]phosphine [3b(T^n)$_2$(D^i−C_6−D^i)$_2$ ≙ II_2]. A mixture of **3b(T^0)** (450 mg, 0.899 mmol), 2 equiv of **D^0−C_6−D^0** (622 mg, 2.112 mmol), water (0.5 mL, 27.778 mmol), and $(n\text{-Bu})_2Sn(OAc)_2$ (27 mg, 0.077 mmol) in 5 mL of MeOH was sol−gel processed: yield 720 mg (95.6%); ^{31}P CP/MAS NMR δ −35.5; ^{13}C CP/MAS NMR δ 70.9 ($PCH_2\mathit{C}H_2OCH_3$), 58.2 ($PCH_2CH_2\mathit{O}CH_3$), 49.8 ($SiOCH_3$), 33.4 [$P(CH_2)_2\mathit{C}H_2\mathit{C}H_2(CH_2)_2Si$, $Si(CH_2)_2\mathit{C}H_2\mathit{C}H_2(CH_2)_2Si$], 27.1 [$P\mathit{C}H_2CH_2OCH_3$, $P(\mathit{C}H_2)_2(CH_2)_4Si$], 23.4 [$P(CH_2)_4\mathit{C}H_2CH_2Si$, $SiCH_2\mathit{C}H_2(CH_2)_2\mathit{C}H_2CH_2Si$], 18.0 [$Si\mathit{C}H_2(CH_2)\mathit{C}H_2Si$], 14.1 [$P(CH_2)_5\mathit{C}H_2Si$], 0.0 ($SiCH_3$); ^{29}Si CP/MAS NMR (silicon substructure) δ −2.4 (D^0), −12.7 (D^1), −22.5 (D^2), −58.8 (T^2), −67.5 (T^3). N_2 surface area: 2.02 m^2/g. Anal. Calcd for $C_{31}H_{67}O_6PSi_4$ (idealized stoichiometry): C, 48.52; H, 8.80. Corrected stoichiometry:[59] C, 47.99; H, 8.91. Found: C, 48.44; H, 8.64.

(2-Methoxyethyl)bis[polysiloxanylhexyl]phosphine [3b(T^n)$_2$(D^i−C_6−D^i)$_4$ ≙ II_4]. A mixture of **3b(T^0)** (367 mg, 0.733 mmol), 4 equiv of **D^0−C_6−D^0** (828 mg, 2.811 mmol), water (0.5 mL, 27.778 mmol), and $(n\text{-Bu})_2Sn(OAc)_2$ (27 mg, 0.077 mmol) in 5 mL of MeOH was sol−gel processed: yield 800 mg (95.8%); ^{31}P CP/MAS NMR δ −35.5; ^{13}C CP/MAS NMR δ 70.9 ($PCH_2\mathit{C}H_2OCH_3$), 58.1 ($PCH_2CH_2\mathit{O}CH_3$), 49.8 ($SiOCH_3$), 33.5 [$P(CH_2)_2\mathit{C}H_2\mathit{C}H_2(CH_2)_2Si$, $Si(CH_2)_2\mathit{C}H_2\mathit{C}H_2(CH_2)_2Si$], 27.1 [$P\mathit{C}H_2CH_2OCH_3$, $P(\mathit{C}H_2)_2(CH_2)_4Si$], 23.4 [$P(CH_2)_4\mathit{C}H_2CH_2Si$, $SiCH_2\mathit{C}H_2(CH_2)_2\mathit{C}H_2CH_2Si$], 18.0 [$Si\mathit{C}H_2(CH_2)\mathit{C}H_2Si$], 13.9 [$P(CH_2)_5\mathit{C}H_2Si$], 0.0 ($SiCH_3$); ^{29}Si CP/MAS NMR (silicon substructure) δ −2.4 (D^0), −12.7 (D^1), −22.5 (D^2), −59.1 (T^2), −67.7 (T^3). N_2 surface area: 1.86 m^2/g. Anal. Calcd for $C_{47}H_{103}O_6PSi_4$ (idealized stoichiometry): C, 48.16; H, 8.86. Corrected stoichiometry:[59] C, 47.88; H, 8.89. Found: C, 45.46; H, 8.07.

(2-Methoxyethyl)bis[methylpolysiloxanylhexyl]phosphine [3c(D^i)$_2$(D^i−C_6−D^i)$_4$ ≙ III_4]. A mixture of **3c(D^0)** (630 mg, 1.344 mmol), 4 equiv of **D^0−C_6−D^0** (1.583 g, 5.376 mmol), water (0.75 mL, 41.167 mmol), and $(n\text{-Bu})_2Sn(OAc)_2$ (27 mg, 0.077 mmol) in 5 mL of MeOH was sol−gel processed: yield 1.50 g (94.1%); ^{31}P CP/MAS NMR δ −35.4; ^{13}C CP/MAS NMR δ 59.0 ($PCH_2CH_2\mathit{O}CH_3$), 50.1 ($SiOCH_3$), 33.5 [$P(CH_2)_2\mathit{C}H_2\mathit{C}H_2(CH_2)_2Si$, $Si(CH_2)_2\mathit{C}H_2\mathit{C}H_2(CH_2)_2Si$], 23.5 [$P(\mathit{C}H_2)_2(CH_2)_4Si$, $P(CH_2)_4\mathit{C}H_2CH_2Si$, $SiCH_2\mathit{C}H_2(CH_2)_2\mathit{C}H_2CH_2Si$], 18.5 [$Si\mathit{C}H_2(CH_2)\mathit{C}H_2Si$, $P(CH_2)_5\mathit{C}H_2Si$], 0.2 ($SiCH_3$), −5.2 [$Si\mathit{C}H_3(OMe)_2$]; ^{29}Si CP/MAS NMR (silicon substructure) δ −2.1 (D^0), −13.7 (D^1), −22.2 (D^2). N_2 surface area: 1.84 m^2/g. Anal. Calcd for $C_{49}H_{109}O_{11}PSi_{10}$ (idealized stoichiometry): C, 49.61; H, 9.26. Corrected stoichiometry:[59] C, 49.65; H, 9.65. Found: C, 48.95; H, 9.32.

(2-Methoxyethyl)bis[polysiloxanyloctyl]phosphine [3d(T^n)$_2$(D^i−C_6−D^i) ≙ IV_1]. A mixture of **3d(T^0)** (549 mg, 0.986 mmol), 1 equiv of **D^0−C_6−D^0** (316 mg, 1.072 mmol), water (0.5 mL, 27.778 mmol), and $(n\text{-Bu})_2Sn(OAc)_2$ (27 mg, 0.077 mmol) in 5 mL of MeOH was sol−gel processed: yield 539 mg (85.6%); ^{31}P CP/MAS NMR δ −36.0; ^{13}C CP/MAS NMR δ 66.8 ($PCH_2\mathit{C}H_2OCH_3$), 58.8 ($PCH_2CH_2\mathit{O}CH_3$), 50.4 ($SiOCH_3$), 28.3 [$P\mathit{C}H_2CH_2OCH_3$, $P(\mathit{C}H_2)_6(CH_2)_2Si$, $Si(CH_2)_2\mathit{C}H_2\mathit{C}H_2(CH_2)_2Si$], 23.4 [$P(CH_2)_6\mathit{C}H_2CH_2Si$, $SiCH_2\mathit{C}H_2(CH_2)_2\mathit{C}H_2CH_2Si$], 18.4 [$Si\mathit{C}H_2(CH_2)\mathit{C}H_2Si$], 14.6 [$P(CH_2)_5\mathit{C}H_2Si$], 0.3 ($SiCH_3$); ^{29}Si CP/MAS NMR (silicon substructure) δ −2.2 (D^0), −14.0 (D^1), −22.4 (D^2), −58.6 (T^2), −67.0 (T^3). N_2 surface area: 9.50 m^2/g. Anal. Calcd for $C_{27}H_{57}O_6PSi_4$ (idealized stoichiometry): C, 52.22; H, 9.25. Corrected stoichiometry:[59] C, 51.50; H, 9.28. Found: C, 49.16; H, 8.50.

(2-Methoxyethyl)bis[polysiloxanyltetradecyl]phosphine [3e(T^n)$_2$(D^i−C_6−D^i) ≙ V_1]. A mixture of **3e(T^0)** (657 mg, 0.914 mmol), 1 equiv of **D^0−C_6−D^0** (269 mg, 0.914 mmol), water (0.5 mL, 27.778 mmol), and $(n\text{-Bu})_2Sn(OAc)_2$ (27 mg, 0.077 mmol) in 5 mL of MeOH was sol−gel processed: yield 683 mg (95.3%); ^{31}P CP/MAS NMR δ −35.8; ^{13}C CP/MAS NMR δ 58.9 ($PCH_2CH_2\mathit{O}CH_3$), 50.2 ($SiOCH_3$), 30.6 [$P\mathit{C}H_2CH_2OCH_3$, $P(\mathit{C}H_2)_{12}(CH_2)_2Si$, $Si(CH_2)_2\mathit{C}H_2\mathit{C}H_2(CH_2)_2Si$], 23.8 [$P(CH_2)_{12}\mathit{C}H_2CH_2Si$, $SiCH_2\mathit{C}H_2(CH_2)_2\mathit{C}H_2CH_2Si$], 18.4 [$Si\mathit{C}H_2(CH_2)\mathit{C}H_2Si$], 14.5 [$P(CH_2)_{13}\mathit{C}H_2Si$], 0.1 ($SiCH_3$); ^{29}Si CP/MAS NMR (silicon substructure) δ −14.1 (D^1), −23.7 (D^2), −60.3 (T^2), −68.8 (T^3). N_2 surface area: 2.28 m^2/g. Anal. Calcd for $C_{39}H_{81}O_6PSi_4$ (idealized stoichiometry): C, 59.34; H, 10.34. Corrected stoichiometry:[59] C, 57.37; H, 10.18. Found: C, 57.88; H, 10.00.

Chlorobis{(2-methoxyethyl)bis[(3-trimethoxysilyl)polysiloxanylpropyl]phosphine-*P*}(η^5-pentamethylcyclopentadienyl)ruthenium(II) [4a(T^n)$_4$(D^i−C_6−D^i) ≙ VI_1]. A mixture of **4a(T^0)** (1.15 g, 1.041 mmol), 1 equiv of **D^0−C_6−D^0** (288 mg, 0.978 mmol), water (0.5 mL, 27.778 mmol), and $(n\text{-Bu})_2Sn(OAc)_2$ (27 mg, 0.077 mmol) in 15 mL of MeOH was sol−gel processed at −20 °C: yield 920 mg (86.8%); ^{31}P CP/MAS NMR δ 14.05; ^{13}C CP/MAS NMR δ 87.2 ($\mathit{C}CH_3$), 68.5 ($PCH_2\mathit{C}H_2OCH_3$), 58.8 ($PCH_2CH_2\mathit{O}CH_3$), 50.5 ($SiOCH_3$), 33.1 [$PCH_2\mathit{C}H_2CH_2Si$, $Si(CH_2)_2\mathit{C}H_2\mathit{C}H_2(CH_2)_2Si$], 27.9 ($P\mathit{C}H_2CH_2OCH_3$), 23.8 [$SiCH_2\mathit{C}H_2(CH_2)_2\mathit{C}H_2CH_2Si$], 18.0 [$P\mathit{C}H_2CH_2\mathit{C}H_2Si$, $SiCH_2(CH_2)_4\mathit{C}H_2Si$], 11.0 ($\mathit{C}CH_3$), 0.3 ($SiCH_3$); ^{29}Si CP/MAS NMR (silicon substructure) δ −2.2 (D^0), −11.8 (D^1), −21.1 (D^2), −42.7 (T^0), −50.1 (T^1), −58.7 (T^2), −67.0 (T^3). N_2 surface area: 0.41 m^2/g. Anal. Calcd for $C_{36}H_{71}ClO_{10}P_2RuSi_6$ (idealized stoichi-

(59) The corrected stoichiometry was obtained by adding the additional number of unhydrolyzed OMe units of the D^0, D^1, D^2, T^0, T^1, T^2, and T^3 groups (obtained from the ^{29}Si CP/MAS NMR spectra) to the idealized stoichoimetry (only D^2 and T^3 units). The real D/T ratios were also taken into account.

ometry): C, 41.94; H, 6.94; Cl, 3.44. Corrected stoichiometry:[59] C, 40.94; H, 7.15; Cl, 3.28. Found: C, 37.50; H, 6.68; Cl, 2.94.

Chlorobis{(2-methoxyethyl)bis[(6-trimethoxysilyl)polysiloxanylhexyl]phosphine-*P*}(η^5-pentamethylcyclopentadienyl)ruthenium(II) [4b(T^n)$_4$ ≙ VII$_0$]. A mixture of **4a(T^0)** (870 mg, 0.739 mmol), water (0.5 mL, 27.778 mmol), and (n-Bu)$_2$Sn(OAc)$_2$ (27 mg, 0.077 mmol) in 5 mL of MeOH was sol−gel processed at −20 °C: yield 620 mg (84.2%); ^{31}P CP/MAS NMR δ 14.2; ^{13}C CP/MAS NMR δ 87.6 (CCH_3), 69.2 ($PCH_2CH_2OCH_3$), 59.0 ($PCH_2CH_2OCH_3$), 50.6 ($SiOCH_3$), 32.2 [$P(CH_2)_2CH_2CH_2(CH_2)_2Si$], 23.8 [$P(CH_2)_2(CH_2)_2(CH_2)_2Si$], 11.0 ($CCH_3$); ^{29}Si CP/MAS NMR (silicon substructure) δ −59.5 (T^2), −67.6 (T^3). N_2 surface area: 5.23 m^2/g. Anal. Calcd for $C_{40}H_{77}ClO_8P_2RuSi_4$ (idealized stoichiometry): C, 48.95; H, 7.79; Cl, 3.56. Corrected stoichiometry:[59] C, 47.61; H, 7.91; Cl, 3.34. Found: C, 45.30; H, 7.08; Cl, 3.73.

Chlorobis{(2-methoxyethyl)bis[(6-trimethoxysilyl)polysiloxanylhexyl]phosphine-*P*}(η^5-pentamethylcyclopentadienyl)ruthenium(II) [4b(T^n)$_4$(D^i−C_6−D^i) ≙ VII$_1$]. A mixture of **4b(T^0)** (3.03 g, 2.380 mmol), 1 equiv of **D^0−C_6−D^0** (701 mg, 2.380 mmol), water (0.5 mL, 27.778 mmol), and (n-Bu)$_2$Sn(OAc)$_2$ (27 mg, 0.077 mmol) in 10 mL of MeOH was sol−gel processed at −20°: yield 2.50 g (87.6%); ^{31}P CP/MAS NMR δ 14.5; ^{13}C CP/MAS NMR δ 87.1 (CCH_3), 69.1 ($PCH_2CH_2OCH_3$), 58.1 ($PCH_2CH_2OCH_3$), 49.9 ($SiOCH_3$), 32.3 [$P(CH_2)_2CH_2CH_2(CH_2)_2Si$, $Si(CH_2)_2CH_2CH_2(CH_2)_2Si$], 23.8 [$PCH_2CH_2(CH_2)_2CH_2CH_2Si$, $SiCH_2CH_2(CH_2)_2CH_2CH_2Si$], 13.7 [$P(CH_2)_5CH_2Si$, $SiCH_2(CH_2)_4CH_2Si$], 11.0 (CCH_3), −0.3 ($SiCH_3$); ^{29}Si CP/MAS NMR (silicon substructure) δ −2.1 (D^0), −11.6 (D^1), −20.9 (D^2), −42.1 (T^0), −49.9 (T^1), −58.6 (T^2), −66.4 (T^3). N_2 surface area: 2.57 m^2/g. Anal. Calcd for $C_{48}H_{95}ClO_{10}P_2RuSi_6$ (idealized stoichiometry): C, 48.07; H, 7.98; Cl, 2.96. Corrected stoichiometry:[59] C, 47.14; H, 8.11; Cl, 2.81. Found: C, 43.78; H, 7.65; Cl 2.73.

Chlorobis{(2-methoxyethyl)bis[(8-trimethoxysilyl)polysiloxanyloctyl]phosphine-*P*}(η^5-pentamethylcyclopentadienyl)ruthenium(II) [4d(T^n)$_4$(D^i−C_6−D^i) ≙ VIII$_1$]. A mixture of **4d(T^0)** (1.386 g, 1.000 mmol), 1 equiv of **D^0−C_6−D^0** (274 mg, 0.930 mmol), water (0.5 mL, 27.778 mmol), and (n-Bu)$_2$Sn(OAc)$_2$ (27 mg, 0.077 mmol) in 5 mL of MeOH was sol−gel processed at −20 °C: yield 1.05 g (80.9%); ^{31}P CP/MAS NMR δ 14.5; ^{13}C CP/MAS NMR δ 87.1 (CCH_3), 69.3 ($PCH_2CH_2OCH_3$), 58.0 ($PCH_2CH_2OCH_3$), 50.1 ($SiOCH_3$), 29.8 [$P(CH_2)_2(CH_2)_4(CH_2)_2Si$, $Si(CH_2)_2CH_2CH_2(CH_2)_2Si$], 23.3 [$PCH_2CH_2(CH_2)_2CH_2CH_2Si$, $SiCH_2CH_2(CH_2)_2CH_2CH_2Si$], 17.9 [$SiCH_2(CH_2)_4CH_2Si$], 13.9 [$P(CH_2)_7CH_2Si$], 10.6 ($CCH_3$), −0.5 ($SiCH_3$); ^{29}Si CP/MAS NMR (silicon substructure) δ −2.4 (D^0), −21.8 (D^2), −50.2 (T^1), −58.9 (T^2), −67.1 (T^3). N_2 surface area: 0.47 m^2/g. Anal. Calcd for $C_{56}H_{111}ClO_{10}P_2RuSi_6$ (idealized stoichiometry): C, 51.29; H, 8.53; Cl, 2.70. Corrected stoichiometry:[59] C, 50.54; H, 8.60; Cl, 2.73. Found: C, 49.38; H, 8.31; Cl, 2.78.

Chlorobis{(2-methoxyethyl)bis[(14-trimethoxysilyl)-polysiloxanyltetradecyl]phosphine-*P*}(η^5-pentamethylcyclopentadienyl)ruthenium(II) [4e(T^n)$_4$(D^i−C_6−D^i) ≙ IX$_1$]. A mixture of **4e(T^0)** (1.427 g, 0.829 mmol), 1 equiv of **D^0−C_6−D^0** (305 mg, 1.036 mmol), water (0.5 mL, 27.778 mmol), and (n-Bu)$_2$Sn(OAc)$_2$ (27 mg, 0.077 mmol) in 5 mL of MeOH was sol−gel processed at −20 °C: yield 1.15 g (81.7%); ^{31}P CP/MAS NMR δ 13.9; ^{13}C CP/MAS NMR δ 58.2 ($PCH_2CH_2OCH_3$), 49.7 ($SiOCH_3$), 30.1 [$P(CH_2)_2(CH_2)_{10}(CH_2)_2Si$, $Si(CH_2)_2(CH_2)_2(CH_2)_2Si$], 23.4 [$PCH_2CH_2(CH_2)_{10}CH_2CH_2Si$, $SiCH_2CH_2(CH_2)_2CH_2CH_2Si$], 17.9 [$SiCH_2(CH_2)_4CH_2Si$], 13.9 [$SiCH_2(CH_2)_4CH_2Si$, $P(CH_2)_{13}CH_2Si$], −0.5 ($SiCH_3$); ^{29}Si CP/MAS NMR (silicon substructure) δ −23.7 (D^2), −60.8 (T^2), −68.8 (T^3). N_2 surface area: 1.43 m^2/g. Anal. Calcd for $C_{80}H_{159}ClO_{10}P_2RuSi_6$ (idealized stoichiometry): C, 58.30; H, 9.72; Cl, 2.15. Corrected stoichiometry:[59] C, 57.78; H, 9.75; Cl, 2.12. Found: C, 55.10; H, 9.10; Cl, 2.05.

Acetonitrilebis{(2-methoxyethyl)bis[(6-trimethoxysilyl)polysiloxanylhexyl]phosphine-*P*}(η^5-pentamethylcyclopentadienyl)ruthenium(II) Hexafluoroantimonate [5b(T^n)$_4$(D^i−C_6−D^i)$_4$ ≙ X$_4$]. A mixture of **5b(T^0)** (1.03 g, 0.680 mmol), 4 equiv of **D^0−C_6−D^0** (745 mg, 2.529 mmol), water (0.5 mL, 27.778 mmol), and (n-Bu)$_2$Sn(OAc)$_2$ (27 mg, 0.077 mmol) in 5 mL of MeOH and 5 mL of $NCCH_3$ was sol−gel processed at −20 °C: yield 1.32 g; IR (KBr, cm^{-1}) ν(CN) 2261 (w); ^{31}P CP/MAS NMR δ 15.32; ^{13}C CP/MAS NMR δ 127.7 ($NCCH_3$), 90.9 (CCH_3), 68.4 ($PCH_2CH_2OCH_3$), 58.3 ($PCH_2CH_2OCH_3$), 49.9 ($SiOCH_3$), 33.1 [$P(CH_2)_2CH_2CH_2(CH_2)_2Si$, $Si(CH_2)_2CH_2CH_2(CH_2)_2Si$], 27.0 [$PCH_2CH_2$], 23.2 [$PCH_2CH_2(CH_2)_2CH_2CH_2Si$, $SiCH_2CH_2(CH_2)_2CH_2CH_2Si$], 17.7 [$SiCH_2(CH_2)_4CH_2Si$], 13.7 [$P(CH_2)_5CH_2Si$], 10.3 ($CCH_3$), 3.5 [$NCCH_3$], −0.4 ($SiCH_3$), −5.6 [$(H_3CO)_2SiCH_3$]; ^{29}Si CP/MAS NMR (silicon substructure) δ −3.5 (D^0), −13.5 (D^1), −23.6 (D^2), −60.3 (T^2), −69.0 (T^3). N_2 surface area: 0.47m^2/g. Anal. Calcd for $C_{54}H_{116}F_6NO_{14}P_2RuSbSi_4$: C, 42.82; H, 7.52; N, 0.93. Corrected stoichiometry:[59] C, 42.37; H, 7.25; N, 0.80. Found: C, 42.74; H, 7.71; N, 0.66.

Acknowledgment. The support of this research by the Deutsche Forschungsgemeinschaft (Forschergruppe, Grant Li 154/41-3/4), Bonn/Bad Godesberg, and by the Fonds der Chemischen Industrie, Frankfurt/Main, is gratefully acknowledged. Furthermore, we thank HASYLAB at DESY, Hamburg, for the provision of synchroton radiation and for technical support, Prof. K. G. Nickel, Institut für Mineralogie, University of Tübingen, for BET measurements, and Dorothea Adam, Institut für Angewandte Physik, University of Tübingen, for SEM measurements.

Supporting Information Available: Detailed synthetic procedures and characterization data for the synthesis of the monomers **3b,d,e(T^0)**, **3c(D^0),** and **4b,d,e(T^0)**. This material is available free of charge via the Internet at http://pubs.acs.org.

CM9900498